Shell-model study of nuclear weak rates relevant to astrophysical processes in stars

Toshio Suzuki
Nihon University

13th Spring Seminar
Ischia, May 17, 2022

Electron-capture and beta-decay rates in stellar environments

1. sd-shell: GT transitions, Nuclear Urca processes
   pf-shell: GT transitions, Synthesis of iron-group elements in Type Ia SN

2. sd-pf shell nuclei: island of inversion, nuclear Urca pair with A=31
   Nuclear Urca processes in neutron star crusts

3. pf-sdg shell: around N=50, ^{78}Ni
   First-forbidden transitions, Core-collapse processes

4. Second-forbidden transitions in ^{20}Ne
   Multipole expansion method by Walecka vs Behrens-Buhring method
   Heating of ONeMg core and its final fate, core-collapse ECSN or thermonuclear ECSN

1a. URCA processes in sd-shell nuclei (USDB)

→ Cooling of O-Ne-Mg core in 8-10 $M_\odot$ stars

e-capture: ${}^{A}_{Z}X + e^- \rightarrow {}^{A}_{Z-1}Y + \nu$ rates increase as density increases

β-decay: ${}^{A}_{Z-1}Y \rightarrow {}^{A}_{Z}X + e^- + \bar{\nu}$ rates decrease as density increases

They occur simultaneously at certain density (URCA density) where both rates are balanced.

Energy is lost from stars by emissions of ν and $\bar{\nu}$ → Cooling of stars.

(^{23}Ne, ^{23}Na) (^{25}Na, ^{25}Mg) Cooling of ONeMg core

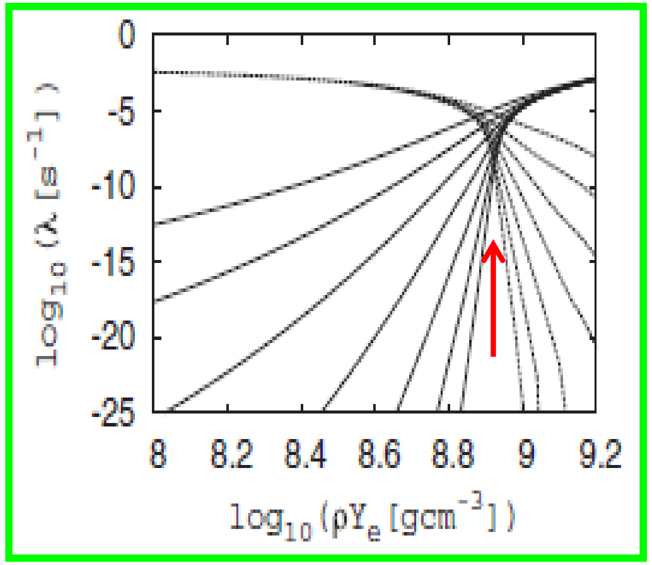

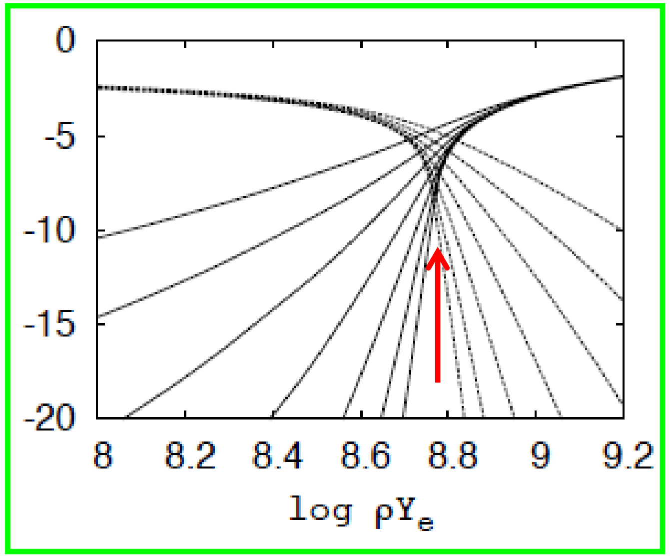

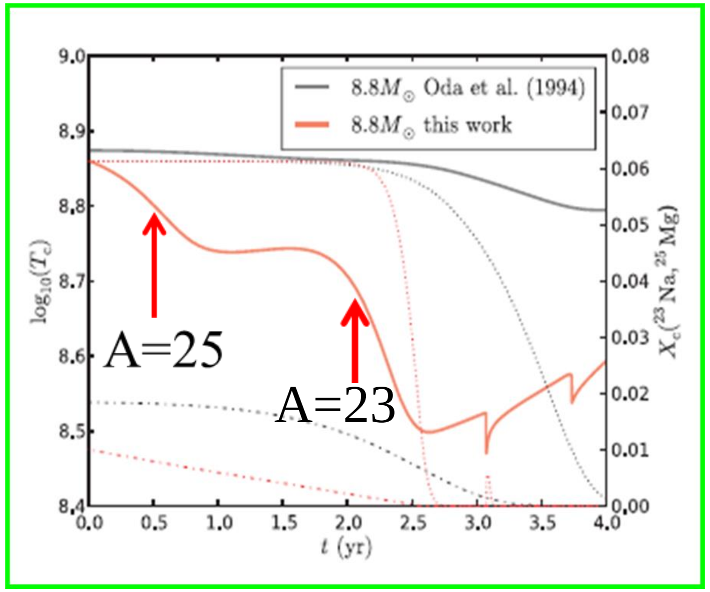

URCA density at $\log_{10}\rho Y_e = 8.92$ $\log_{10}\rho Y_e = 8.78$

β-decay Q vales: Q=4.376 MeV Q=3.835 MeV

Toki, Suzuki, Nomoto, Jones and Hirschi, PR C 88, 015806 (2013)

1b.Type-Ia SNe and synthesis of iron-group nuclei

e-capture rates: GXP;
GXPF1J ($21 \le Z \le 32$) and KBF (other Z)

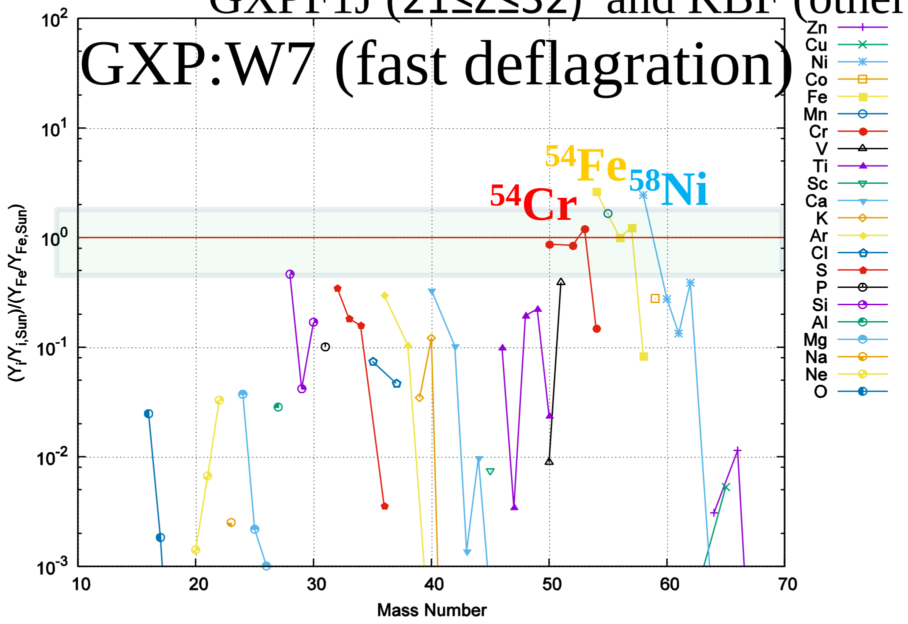

Single-degenerate model: Accretion of matter to white-dwarf (WD) from binary star

SN explosion when WD mass ≈ Chandrasekhar limit
^{56}Ni (e^-, ν) ^{56}Co, $\rightarrow Y_e < 0.5$ (neutron-rich)
→ production of neutron-rich isotopes such as ^{58}Ni

Problem of over-production of neutron-excess iron-group isotopes such as ^{58}Ni, ^{54}Cr … compared with solar abundances for e-capture rates of FFN (Fuller-Fowler-Newman)

GXP: WDD2 (slow deflagration + detonation)

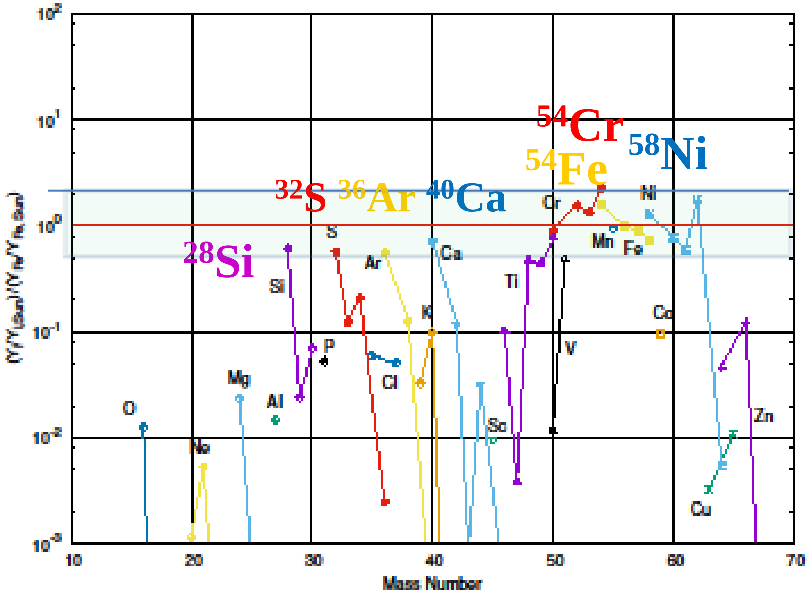

e-capture rates of shell-model with GXPF1J (Honma et al.) and KBF (Langanke& Martinez-Pinedo) in pf-shell
→ Decrease of e-capture rate and less production of ^{58}Ni
Over-production problem is suppressed within a factor of ~ 2.

Mori, Famiano, Kajino, Suzuki, Hidaka, Honma, Iwamoto, Nomoto, Otsuka, ApJ. 833, 179 (2016)

2.Weak rates for nuclei in the island of inversion

Cooling in neutron star crusts by nuclear URCA processes

Schatz et al, Nature 505, 65 (2014)

Table 1 | Electron-capture/β^--decay pairs with highest cooling rates

Electron-capture/β^--decay pair		Density†	Chemical potential†	Luminosity‡
Parent	Daughter*	(10^{10} g cm^{-3})	(MeV)	(10^{36} erg s^{-1})
^{29}Mg	^{29}Na	4.79	13.3	24
^{55}Ti	^{55}Sc, ^{55}Ca	3.73	12.1	11
^{31}Al	^{31}Mg	3.39	11.8	8.8
^{33}Al	^{33}Mg	5.19	13.4	8.3
56Ti	56Sc	5.57	13.8	3.5

Rates evaluated by QRPA
Shell-model evaluations
are missing.

Island of inversion
Z=10-12, N = 20-22

Neutron-rich Ne, Na, Mg isotopes

- Small shell-gap: $f_{7/2}$-$d_{3/2}$
- Small $E_x(2^+)$
- Large B(E2)

→ Large sd-pf admixture

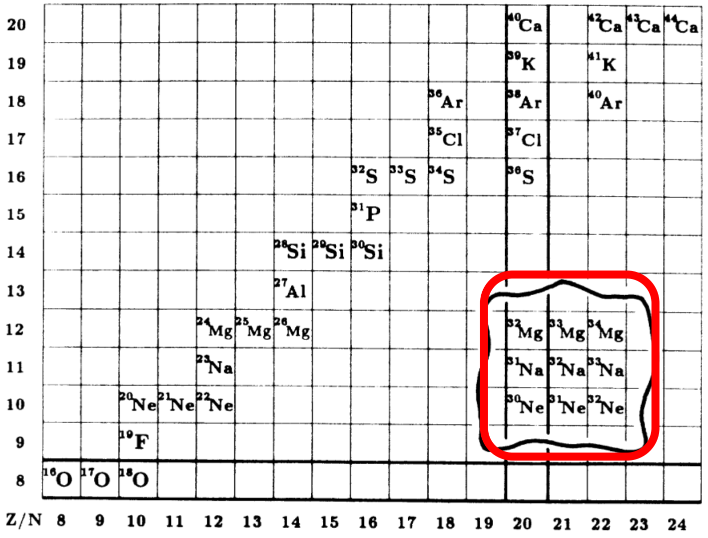

Warburton, Becker, Brown, PR C41, 1147 (1990)

Effects of Tensor Force on Shell Evolution

Neutron ESP for N=20 isotones

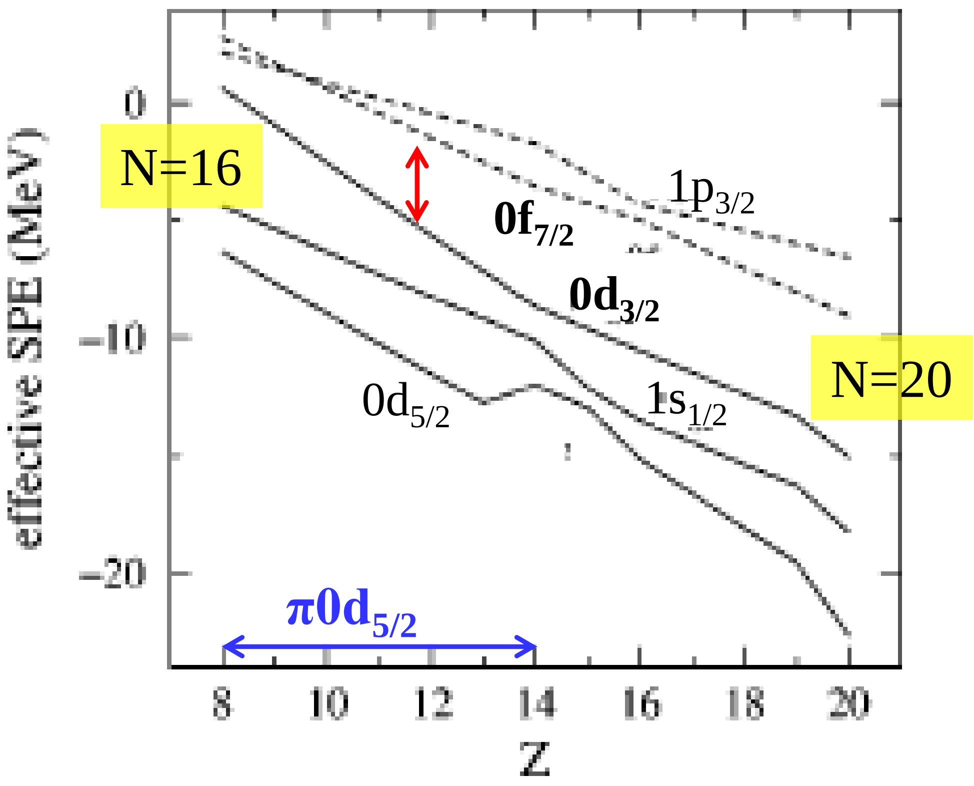

SDPF-M: Utsuno et al., PR C60, 054315 (1999)

Shell-gap ($\nu d_{3/2}$-$\nu f_{7/2}$) decreases for less protons in $d_{5/2}$-shell
→ Magic number changes from N=20 to N=16

Monopole terms
$\pi d_{5/2}$-$\nu d_{3/2}$: attraction
$\pi d_{5/2}$-$\nu f_{7/2}$: repulsion

Otsuka, Suzuki, Fujimoto, Grawe, Akaishi, PRL 69 (2005)

Neutron-rich Ne, Na, Mg isotopes

SDPF-M: Utsuno et al., PR C60, 054315 (1999)

# of nucleons in pf-shell

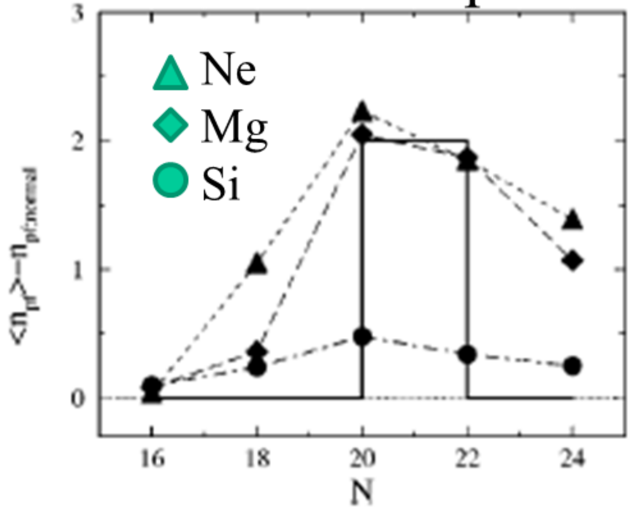

sd-pf admixture

- Small shell-gap: $f_{7/2}$-$d_{3/2}$
- Small $E_x(2^+)$
- Large B(E2)

E_x: 2^+, 4^+ B(E2)

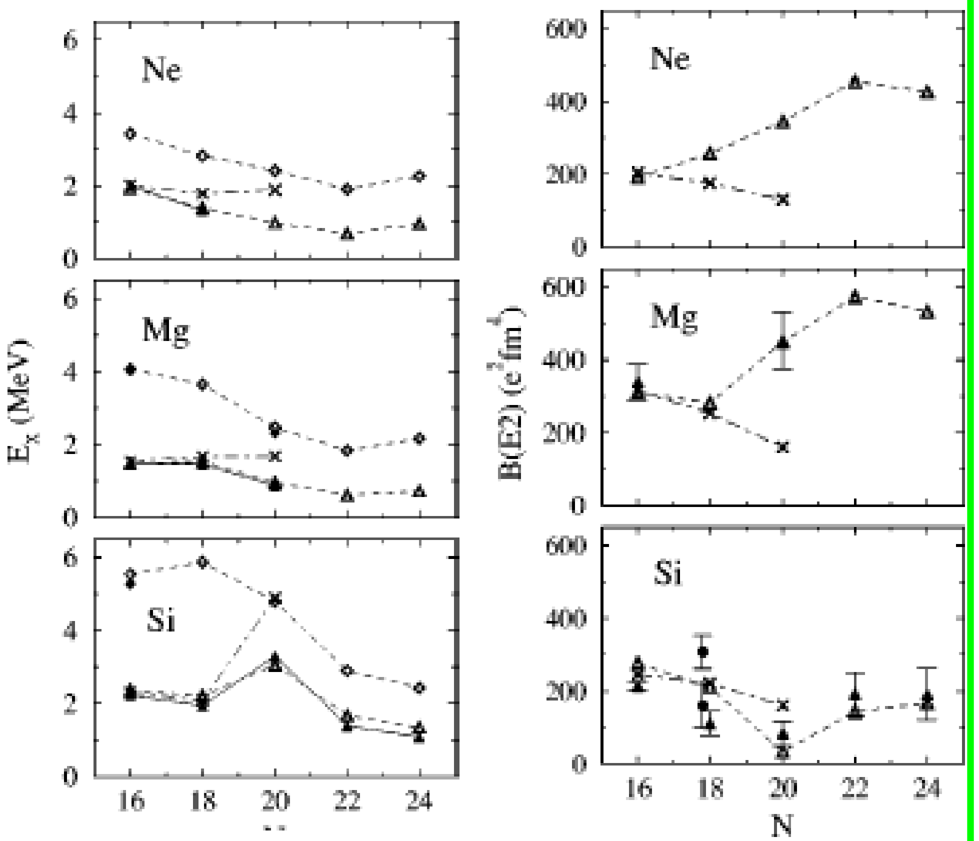

filled =exp. × = sd only

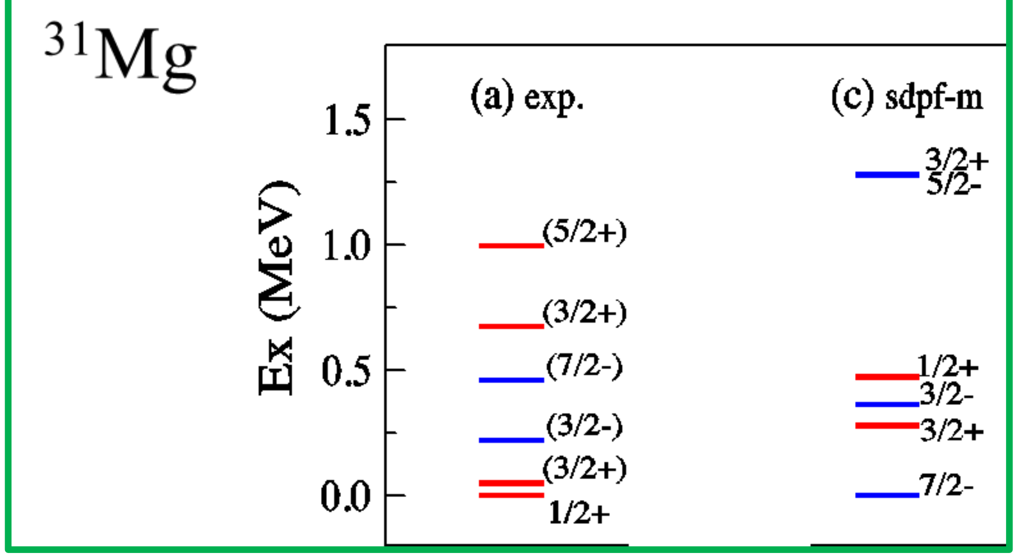

SDPF-M

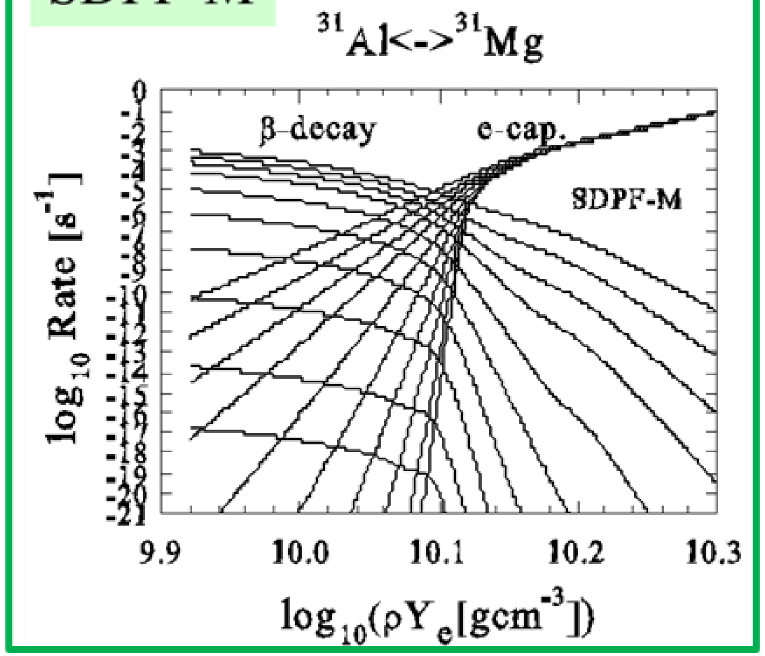

sd-pf shell

Non-degenerate treatment of sd and pf shells by
EKK (extended Kuo-Krenciglowa) method

Tsunoda, Takayanagi, Hjorth-Jensen and Otsuka, Phys. Rev. C 89, 024313 (2014)

Cf: monopoles with non-degenerate vs degenerate method

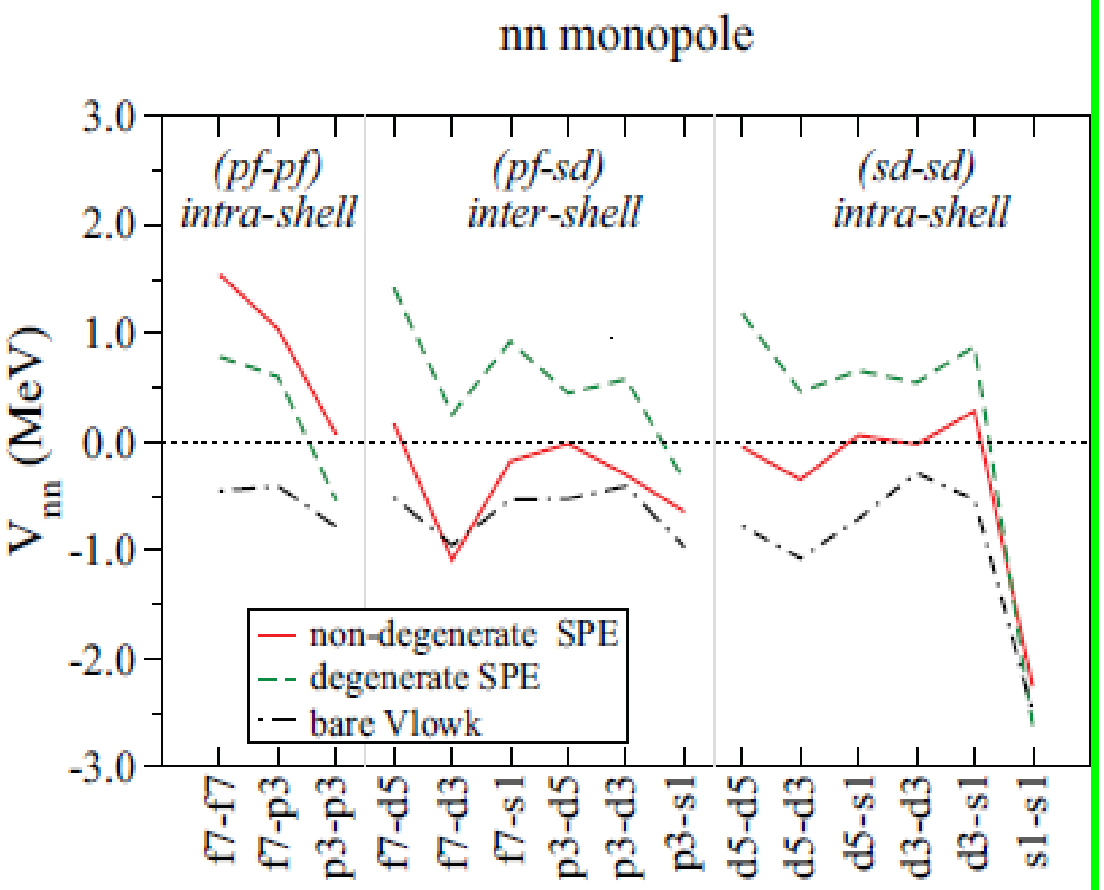

Kuo-Krenciglowa method

$$V_{\rm eff}^{(n)} = \hat{Q}(\epsilon_0) + \sum_{k=1}^{\infty} \hat{Q}_k(\epsilon_0)\{V_{\rm eff}^{(n-1)}\}^k,$$

$$PH_0P = \epsilon_0 P.$$

$$\hat{Q}(E) = PVP + PVQ\frac{1}{E - QHQ}QVP,$$

$$\hat{Q}_k(E) = \frac{1}{k!}\frac{d^k \hat{Q}(E)}{dE^k}.$$

Extended Kuo-Krenciglowa method

$$\tilde{H} = H - E$$

$$\tilde{H}_{\rm eff}^{(n)} = \tilde{H}_{\rm BH}(E) + \sum_{k=1}^{\infty} \hat{Q}_k(E)\{\tilde{H}_{\rm eff}^{(n-1)}\}^k,$$

$$\tilde{H}_{\rm eff} = H_{\rm eff} - E, \quad \tilde{H}_{\rm BH}(E) = H_{\rm BH}(E) - E,$$

$$H_{\rm BH}(E) = PHP - PVQ\frac{1}{E - QHQ}QVP.$$

$$V_{\rm eff} = H_{\rm eff} - PH_0P.$$

energy indpendent

K. Takayanagi, Nucl. Phys. A 852, 61 (2011).
K. Takayanagi, Nucl. Phys. A 864, 91 (2011).

Neutron-rich isotopes in the island of inversion by EKK-method starting from chiral EFT interaction N^3LO+3N (FM)

Tsunoda, Otsuka, Shimizu, Hjorth-Jensen, Takayanagi and Suzuki, PRC 95, 021304(R) (2017)

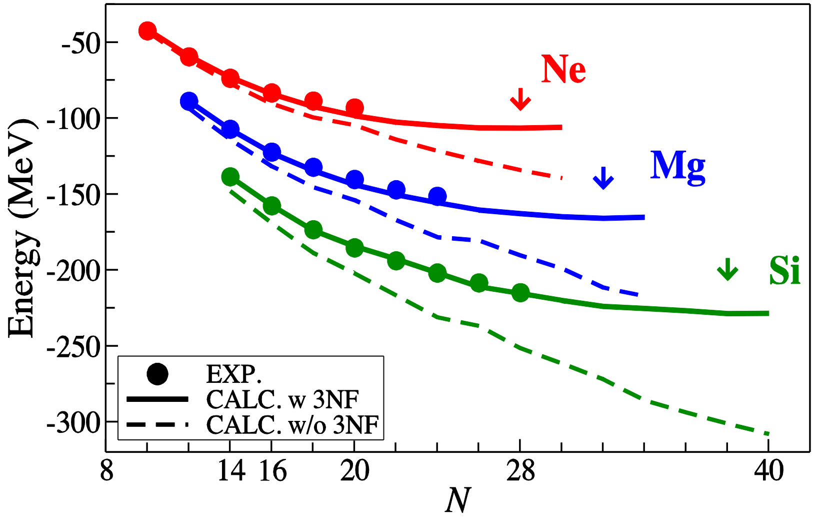

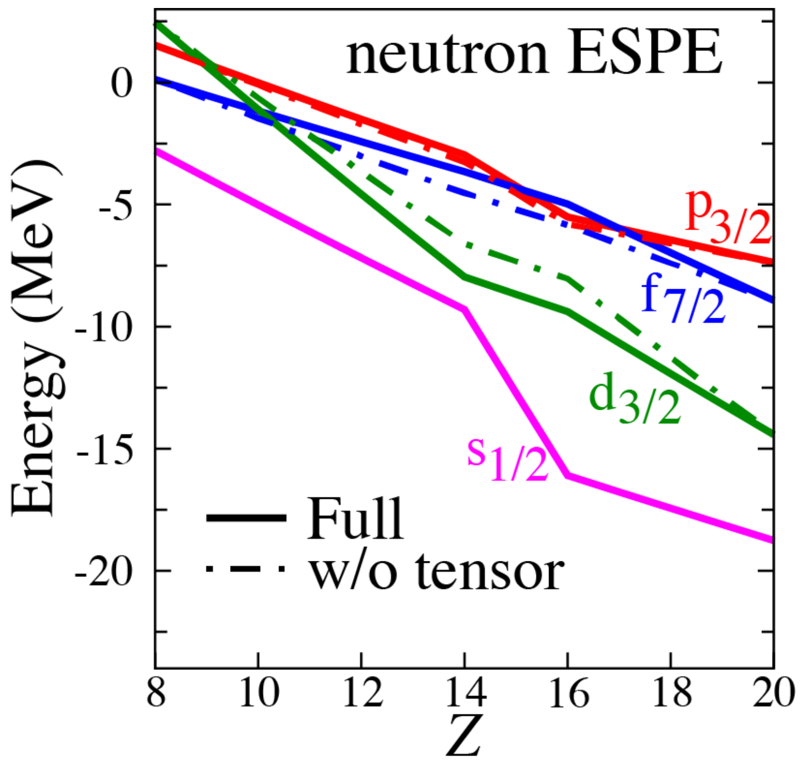

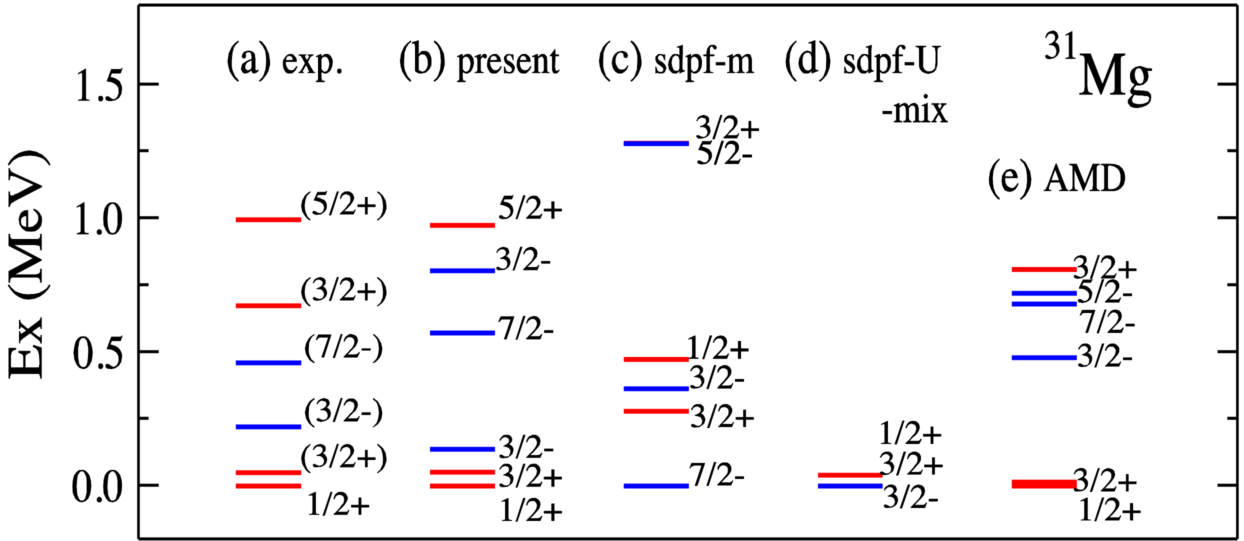

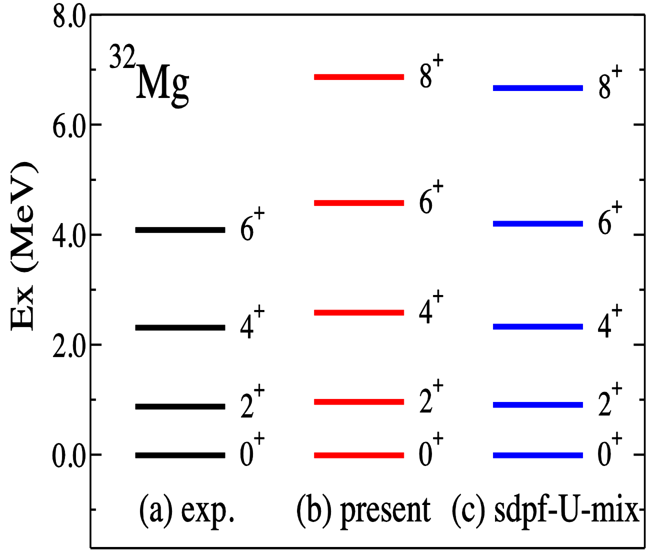

EKK vs EXP

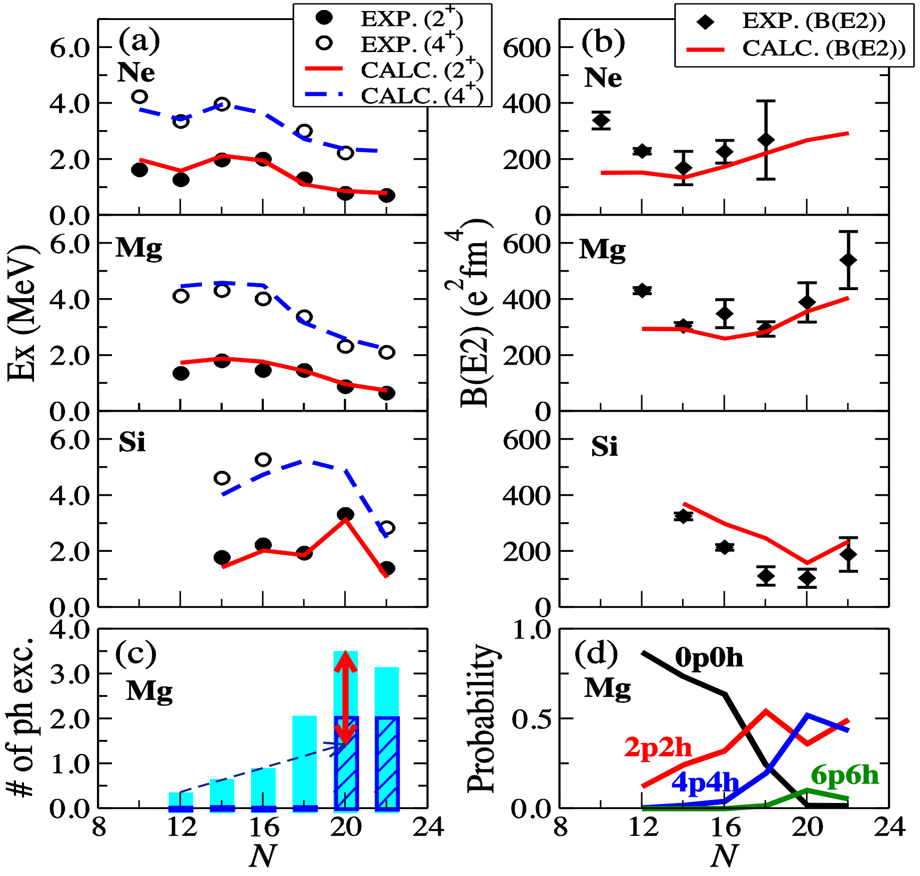

2p-2h+4p-4h

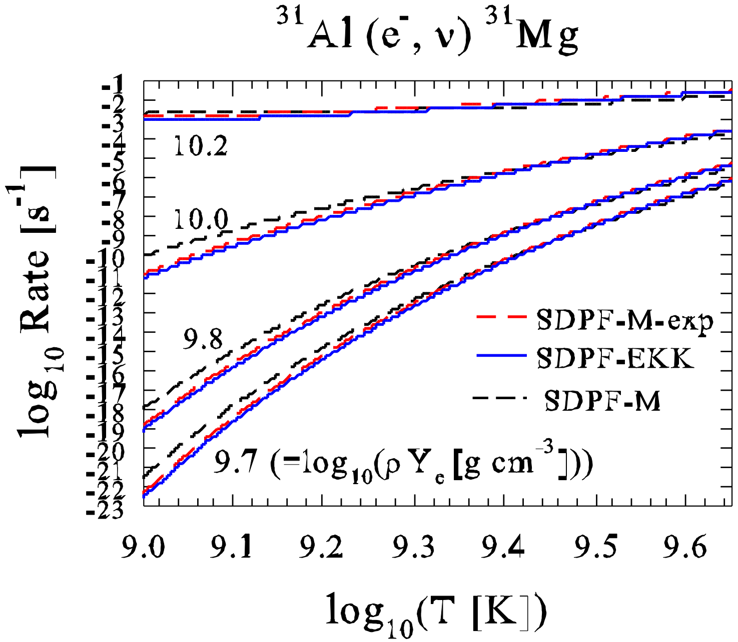

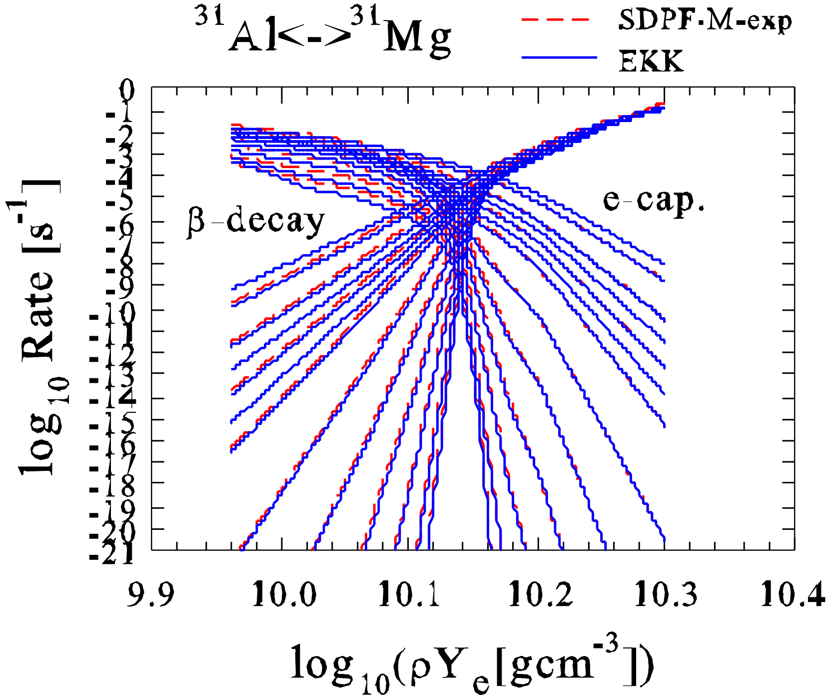

3. Weak rates of pf-g shell nuclei and core-collapse SNe

Which nuclei affect $\dot{Y}_e$(change of Y_e) most in core-collapse process?

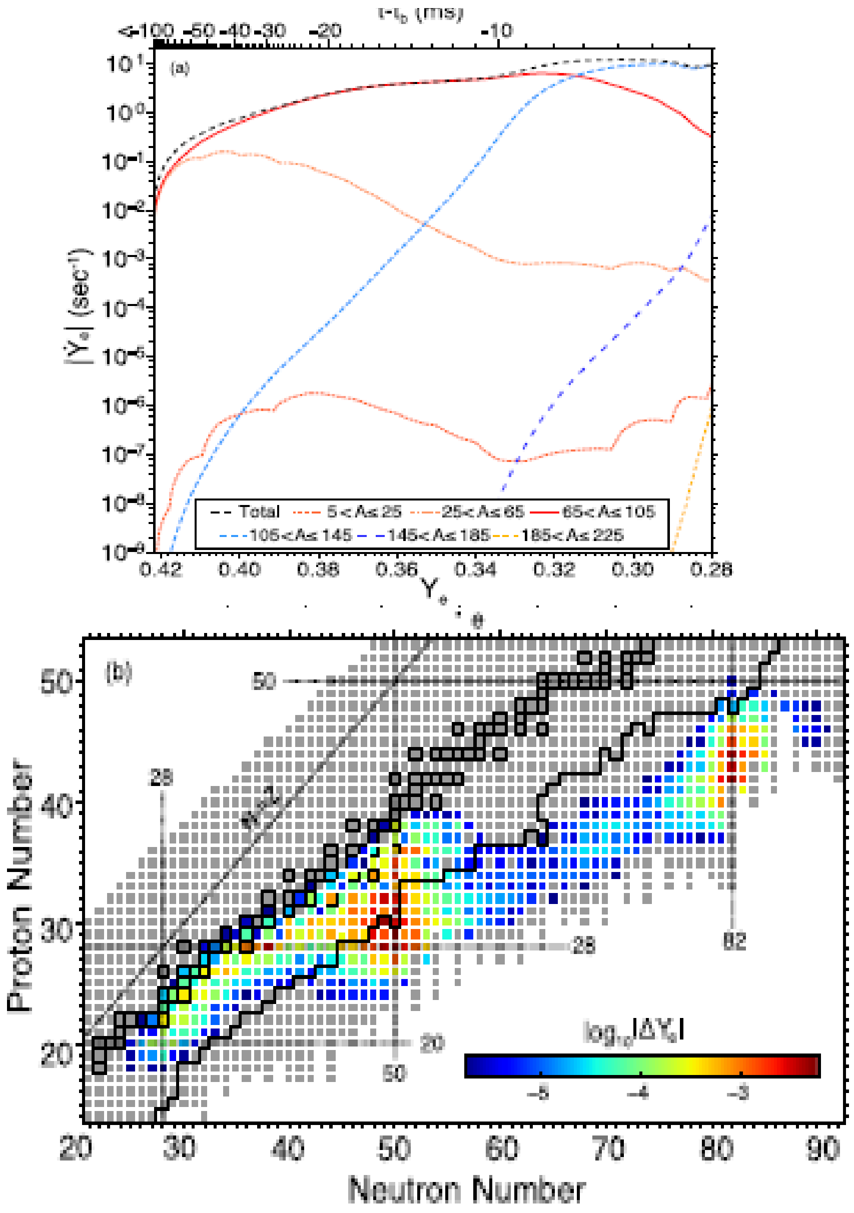

Sullivan et al., ApJ. 816, 44 (2016)

^{78}Ni

- SM (pf-sdg; modified A3DA)

A3DA
pf-$g_{9/2}d_{5/2}$
Y.Tsunoda et al., PRC 89, 031301R (2014)
$E_x(2^+)$ = 2.8 MeV
Up to 5p-5h outside filling config. of ^{78}Ni

→ full pf-gds

- Effective rate formula
- RPA

- Spin-dipole strengths

Spin-dipole strength

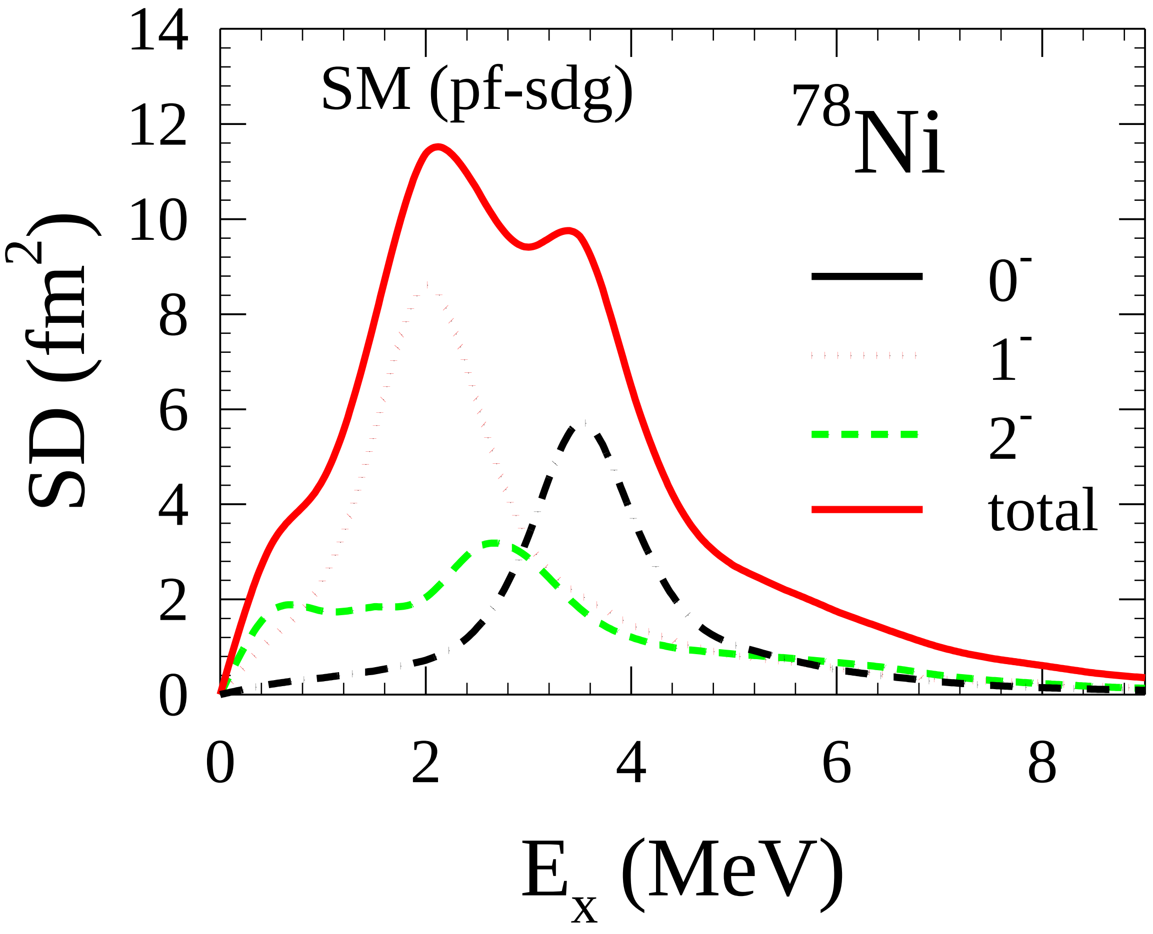

Spin-dipole operator

$$O_m^\lambda = [rY^1(\hat{\vec{r}}) \times \vec{\sigma}]_m^\lambda \, t_+$$

Sum of the strengths

$S=\Sigma_i\langle g.s. |O^+ |i\rangle\langle i|O|g.s.\rangle$

	SM(pf-gds)	RPA (full)
0-	11.60 (95%)	12.38 (fm^2)
1-	19.89 (96%)	20.68
2-	12.57 (79%)	16.00

Cf.

	SM(pf-$g_{9/2}d_{5/2}$)
0-	0.05
1-	1.60
2-	2.62

SM vs RPA vs Effective rate formula

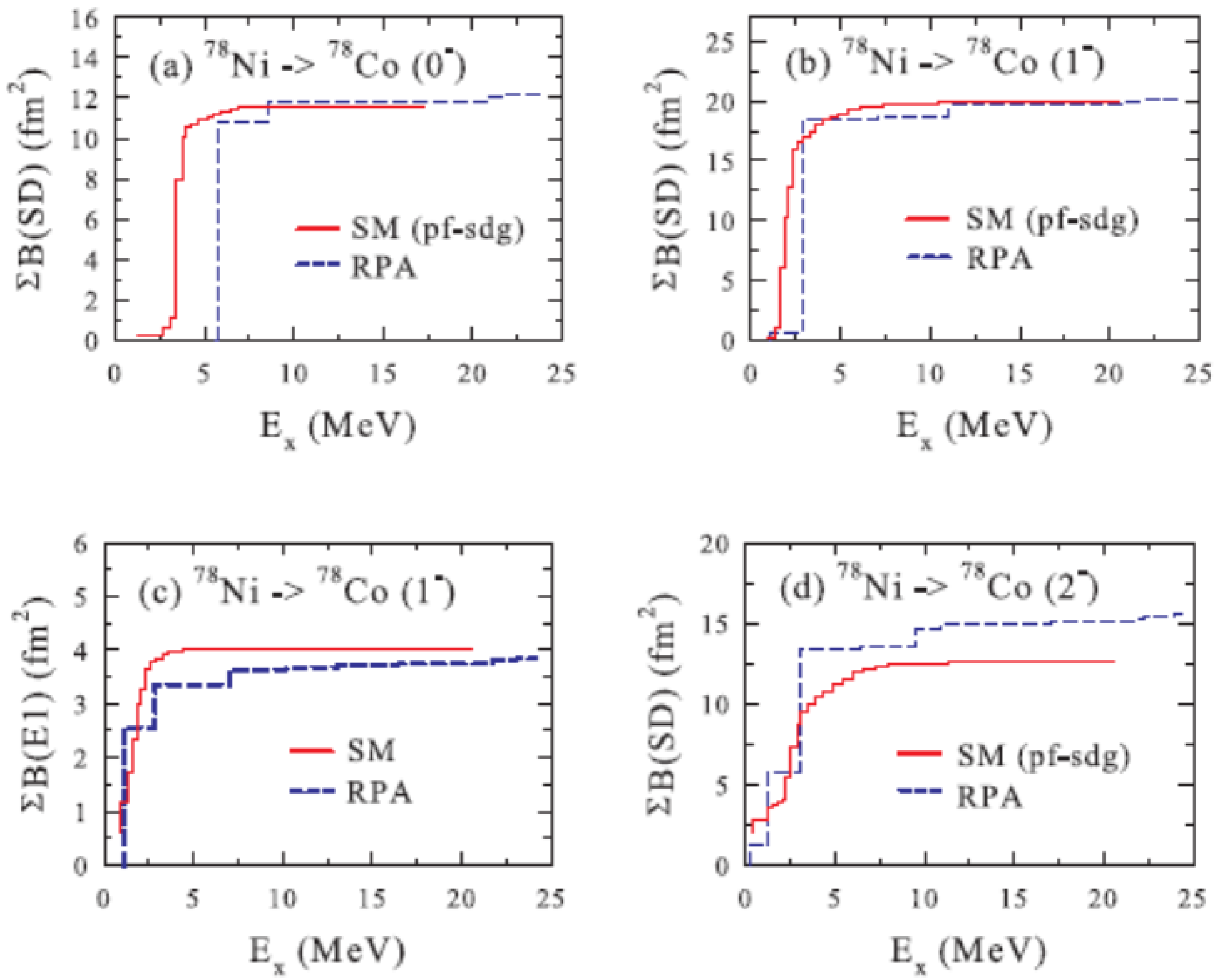

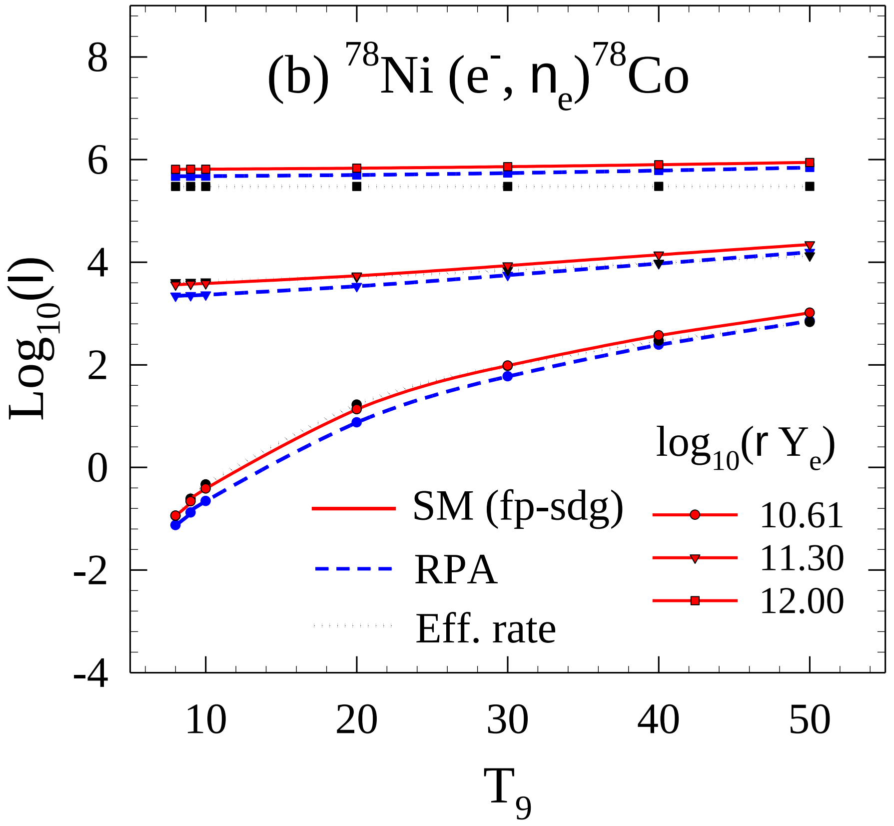

Effective rate formula:

$Q \rightarrow Q - \Delta E$

Effective energy difference $\Delta E = 2.5$ MeV

$$\lambda = \frac{ln2 \cdot B}{K}\left(\frac{T}{m_e c^2}\right)^6 [F_4(\eta) - 2\xi F_3(\eta) + \xi^2 F_2(\eta)]$$

$$F_k(\eta) = -\Gamma(k+1) Li_{k+1}(-e^{\eta})$$

K =6146 s, F_k are Fermi integrals of rank k

$\eta = \xi + \mu_e/T$ with $\xi = (Q - \Delta E)/T$

Multipole expansion method by Walecka (at low q)

$$C_{ecap}^{0^-} = (\xi' v - \frac{1}{3} w W_0)^2$$

$$C_{ecap}^{1^-} = [\xi' y + \frac{1}{3}(u + x) W_0]^2 + \frac{1}{18}(u - 2x)^2$$
$$+ W[-\frac{4}{3}\xi' y u - \frac{W_0}{9}(4x^2 + 5u^2)] + \frac{W^2}{9}(4x^2 + 5u^2)$$

$$\xi' v = -\frac{\sqrt{3}}{\sqrt{2J_i+1}} g_A < f||\frac{1}{M}[\vec{\sigma} \times \vec{\nabla}]^{(0)}||i >$$

$$w = -\frac{\sqrt{3}}{\sqrt{2J_i+1}} g_A < f||r[C^1(\Omega) \times \vec{\sigma}]^{(0)}||i >$$

$$\xi' y = \frac{1}{\sqrt{2J_i+1}} < f||\frac{\vec{\nabla}}{M}||i >$$ **E1**

$$x = \frac{1}{\sqrt{2J_i+1}} < f||r C^1(\Omega)||i >$$ **C1**

$$u = \frac{\sqrt{2}}{\sqrt{2J_i+1}} g_A < f||r[C^1(\Omega) \times \vec{\sigma}]^{(1)}||i >$$ **$M_5$1 (SD1)**

$\xi' y$ =-$\Delta E_{fi} x$ with $\Delta E_{fi} = E_f - E_i$,

Behrens-Buhring method
distorted electron w.f.

$\xi' v \rightarrow \xi' v - \xi w'$ for $\lambda^\pi = 0^-$

$\xi' y \rightarrow \xi' y - \xi(u' - x')$ for $\lambda^\pi = 1^-$

$$\xi = \frac{\alpha Z}{2R}.$$

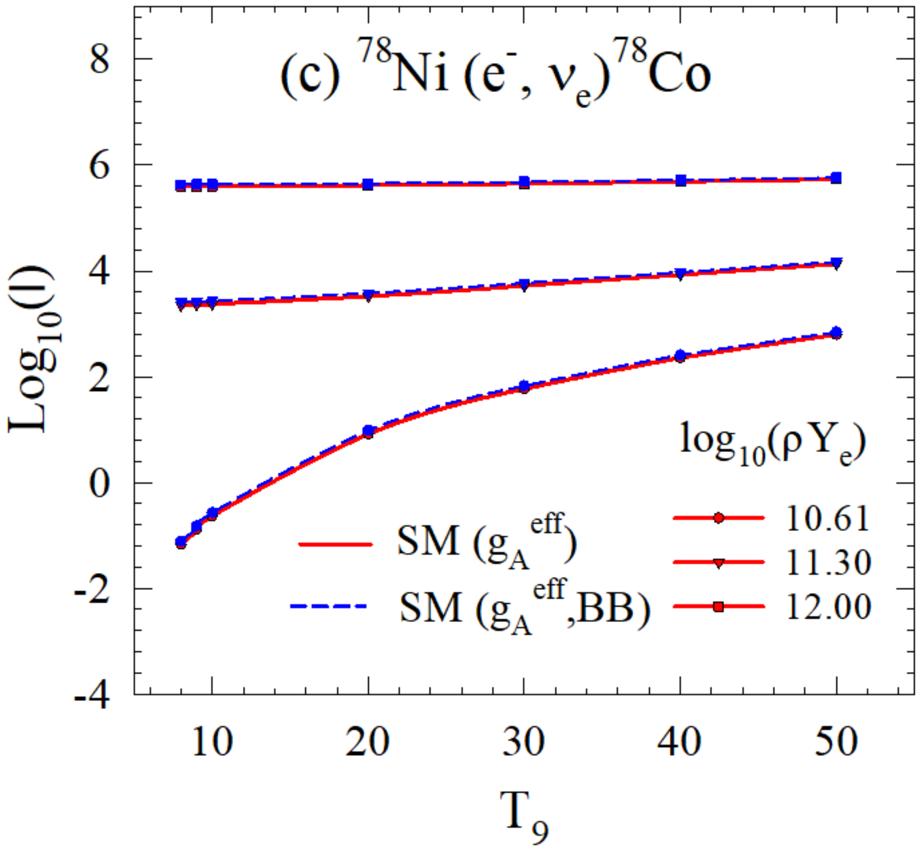

4. Second-forbidden transition in ^{20}Ne and Evolution of ONeMg-core toward e-capture SN

$^{20}Ne\,(e^-, \nu)\,^{20}F$

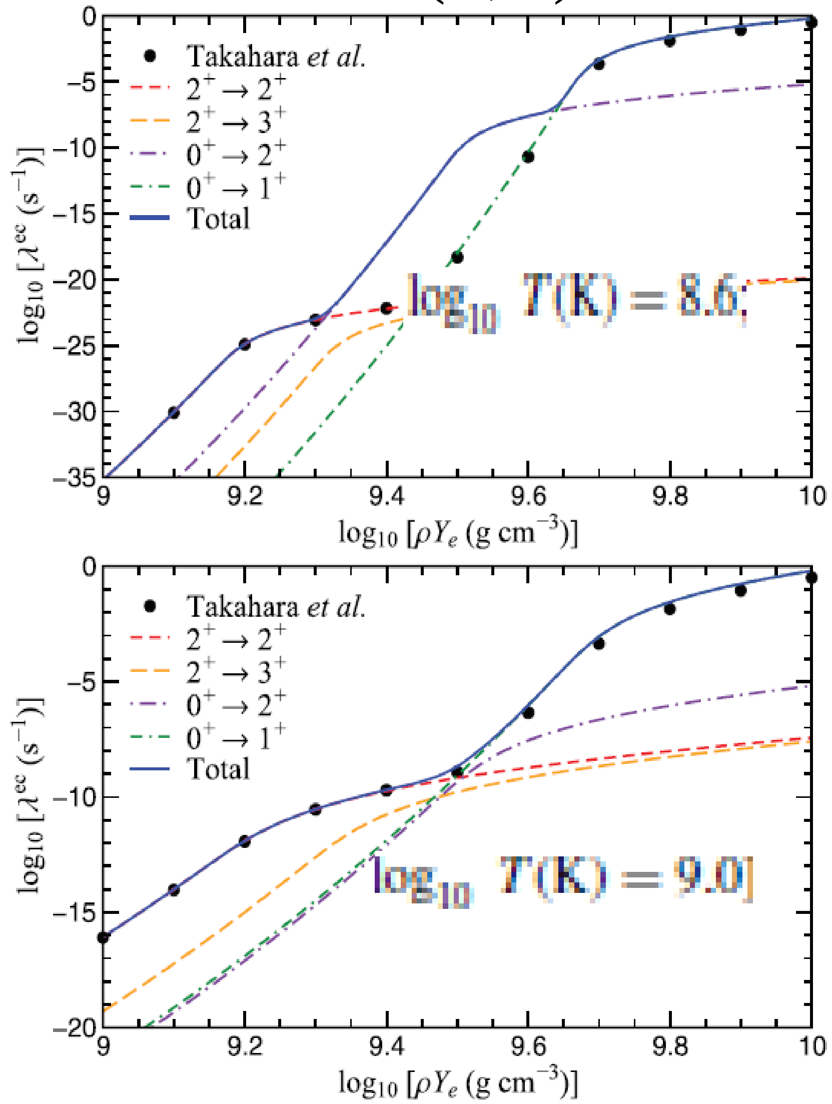

Martinez-Pinedo et al., PR C89, 045806 (2014)

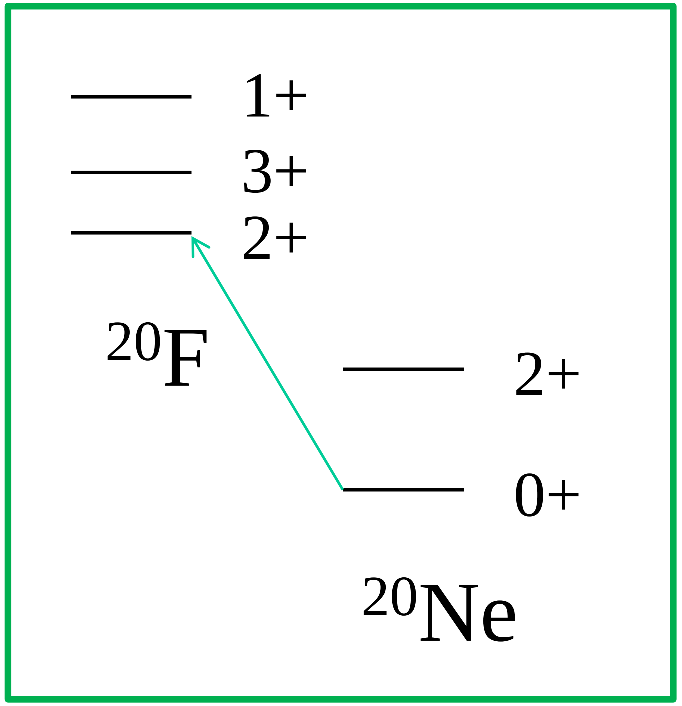

0+ -> 2+: 2nd-forbidden transition

Kirsebom et al., PRL 123, 262701 (2019)

β-decay exp. -> log ft = 10.89(11)

cf. NNDC : log ft > 10.5

$$ft = \frac{6147}{B(GT)} \qquad O_{GT} = g_A \vec{\sigma}\tau_-$$

e-capture rate

$$\lambda^{ecap}(T) = \frac{V_{ud}^2 g_V^2 c}{\pi^2(\hbar c)^3}\int_{E_{th}}^{\infty}\sigma(E_e,T)E_e p_e c S_e(E_e)dE_e$$

$$\sigma(E_e,T) = \sum_i \frac{(2J_i+1)e^{-E_i/kT}}{G(Z,A,T)}\sum_f \sigma_{f,i}(E_e)$$

$$G(Z,A,T) = \sum_i (2J_i+1)e^{-E_i/kT},$$

shape factor

$$\sigma_{f,i}(E_e) = \frac{G_F^2}{2\pi}F(Z,E_e)W(E_\nu)\boxed{C_{f,i}(E_e)}$$

$$W(E_\nu) = \frac{E_\nu^2}{1+E_\nu/M_T}$$

$$\begin{aligned} C_{f,i}(E_e) &= \frac{1}{2J_i+1}\int d\Omega\Big(\sum_{J\geq 1}\{(1-(\hat{\vec{\nu}}\cdot\hat{\vec{q}})(\vec{\beta}\cdot\hat{\vec{q}})[|\langle J_f||T_J^{mag}||J_i\rangle|^2+|\langle J_f||T_J^{elec}||J_i\rangle|^2] \\ &- 2\hat{\vec{q}}\cdot(\hat{\vec{\nu}}-\vec{\beta})Re\langle J_f||T_J^{mag}||J_i\rangle\langle J_f||T_J^{elec}||J_i\rangle^*\} \\ &+ \sum_{J>0}\{(1-\hat{\vec{\nu}}\cdot\vec{\beta})+2(\hat{\vec{\nu}}\cdot\hat{\vec{q}})(\vec{\beta}\cdot\hat{\vec{q}})|\langle J_F||L_J||J_i\rangle|^2+(1+\hat{\vec{\nu}}\cdot\vec{\beta})|\langle J_f||M_J||J_i\rangle|^2 \\ &- 2\hat{\vec{q}}\cdot(\hat{\vec{\nu}}+\vec{\beta})Re\langle J_f||L_J||J_i\rangle\langle J_f||M_J||J_i\rangle^*\}\Big), \end{aligned}$$

$J=2^+$

$$C2+L2:\quad F_1^V\frac{q_\mu^2}{q^2}j_2(qr)Y^2$$

$$E2:\quad \frac{q}{M}[F_1^V(\sqrt{\frac{3}{5}}j_1(qr)[Y^1\times\frac{\nabla}{q}]^2-\sqrt{\frac{2}{5}}j_3(qr)[Y^3\times\frac{\nabla}{q}]^2)+\frac{1}{2}\mu_V j_2(qr)[Y^2\times\sigma]^2$$

$$M2_5:\quad F_A j_2(qr)[Y^2\times\sigma]^2$$

- Low q (momentum transfer) limit

$$
\begin{aligned}
x &= \frac{1}{\sqrt{2J_i+1}}\langle f||r^2 C^2(\Omega)||i\rangle \\
y &= \frac{1}{\sqrt{2J_i+1}}\langle f||r[C^1(\Omega)\times\frac{\vec{\nabla}}{M}]^2||i\rangle \\
u &= \frac{1}{\sqrt{2J_i+1}}g_A\langle f||r^2[C^2(\Omega)\times\vec{\sigma}]^2||i\rangle \\
C(k,\nu) &= \frac{1}{45}x^2(k^4-\frac{4}{3}\beta k^3\nu+\frac{10}{3}k^2\nu^2-\frac{4}{3}\beta k\nu^3+\nu^4)+\frac{2}{15}y^2(k^2-2\beta k\nu+\nu^2) \\
&+ \frac{2}{45}\sqrt{6}xy(\beta k^3-\frac{5}{3}k^2\nu+\frac{5}{3}\beta k\nu^2-\nu^3) \\
&+ \frac{1}{5}y^2(k^2+\nu^2+\frac{4}{3}\beta k\nu)+\frac{1}{45}u^2(k^4+2\beta k^3\nu+\frac{10}{3}k^2\nu^2+2\beta k\nu^3+\nu^4) \\
&- \frac{2}{15}yu(\beta k^3+\frac{5}{3}k^2\nu+\frac{5}{3}\beta k\nu^2+\nu^3).
\end{aligned}
$$

1st line: C2+L2

2nd line: C2-L2 interference

3rd line: E2 + $M2_5$

4th line: E2-$M2_5$ interference

$q \to 0$

$$L_2(q) = \sqrt{\frac{2}{3}} T_2^{elec}(q) = -\frac{i}{q} \sum_k \frac{q^2 r_k^2}{15} \nabla \cdot \mathbf{V}_{\pm,k} Y^2(\Omega_k).$$

de Forest, T. Jr., Walecka, J. D., Adv. in Phys. **15**, 1 (1966),

CVC: conservation of vector current

$$\nabla \cdot \mathbf{V}_\pm = -\frac{\partial \rho_\pm}{\partial t} = -i[H, \rho_\pm]$$

$$\rho_\pm = F_1^V(q^2) \sum_k \delta(\mathbf{r} - \mathbf{r}_k) t_\pm$$

$$\langle J_f || L_2(q) || J_i \rangle = \sqrt{\frac{2}{3}} \langle J_f || T_2(q) || J_i \rangle = -\frac{E_f - E_i}{q} \langle J_f || M_2(q) || J_i \rangle$$

$$y = -\frac{E_f - E_i}{\sqrt{6}\hbar} x.$$

With inclusion of isovector electromagnetic interaction

$\Delta E \equiv E_f - E_i \pm V_C \mp (m_n - m_p).$ = energy of IAS of ^{20}F (2^+) : ^{20}Ne (2^+, 10.274)

Fujita, J., Phys. Rev. **126**, 202 (1962),

Fujita, J., Prog. Theor. Phys. **28**, 338 (1962),

Eichler, J., Z. Phys. **171**, 463 (1963),

Vc = Coulomb energy difference

Behrens-Buring (BB) H. Behrens and W. Buhring, *Nucl. Phys.* A 162 (1971) 111

electron w.f.: plane wave -> distorted wave in a Coulomb pot.

$$
\begin{aligned}
C(k,\nu) &= \frac{\nu^2}{3}\{[y+\sqrt{\frac{2}{3}}x(\frac{E_e}{3}-\frac{\nu}{5})-u(\frac{E_e}{3}+\frac{\nu}{5})+\frac{1}{3}3\xi(\sqrt{\frac{2}{3}}x_1'-u_1')]^2+\frac{1}{9}(\sqrt{\frac{2}{3}}x-u)^2\} \\
&+ \frac{k^2}{3}\{[y+\sqrt{\frac{2}{3}}x(\frac{E_e}{5}-\frac{\nu}{3})-u(\frac{E_e}{5}+\frac{\nu}{3})+\frac{3\xi}{5}(\sqrt{\frac{2}{3}}x_2'-u_2')]^2+\frac{1}{25}(\sqrt{\frac{2}{3}}-u)^2\} \\
&+ \frac{\nu^4}{50}(\sqrt{\frac{2}{3}}x-\frac{2}{3}u)^2+\frac{k^2\nu^2}{27}\frac{2}{3}x^2+\frac{k^4}{50}(\sqrt{\frac{2}{3}}x+\frac{2}{3}u)^2,
\end{aligned}
$$

$\xi = \frac{\alpha Z}{2R}$ coupling between operator and e-w.f.

finite-size effect of Coulomb pot.

$$
\begin{aligned}
x_1' &= \frac{1}{\sqrt{2J_i+1}}\langle f||r^2C^2(\Omega)I(1,1,1,1;r)||i\rangle \\
x_2' &= \frac{1}{\sqrt{2J_i+1}}\langle f||r^2C^2(\Omega)I(2,1,1,1;r)||i\rangle \\
u_1' &= \frac{1}{\sqrt{2J_i+1}}g_A\langle f||r^2[C^2(\Omega)\times\vec{\sigma}]^2I(1,1,1,1;r)||i\rangle \\
u_2' &= \frac{1}{\sqrt{2J_i+1}}g_A\langle f||r^2[C^2(\Omega)\times\vec{\sigma}]^2I(2,1,1,1;r)||i\rangle \\
I(k,1,1,1;r) &= \begin{cases} \frac{2}{3}\{\frac{3}{2}-\frac{2k+1}{2(2k+3)}(\frac{r}{R})^2\} & r\le R \\ \frac{2}{3}\{\frac{2k+1}{2k}\frac{R}{r}-\frac{3}{2k(2k+3)}(\frac{R}{r})^{2k+1}\} & r\ge R \end{cases}
\end{aligned}
$$

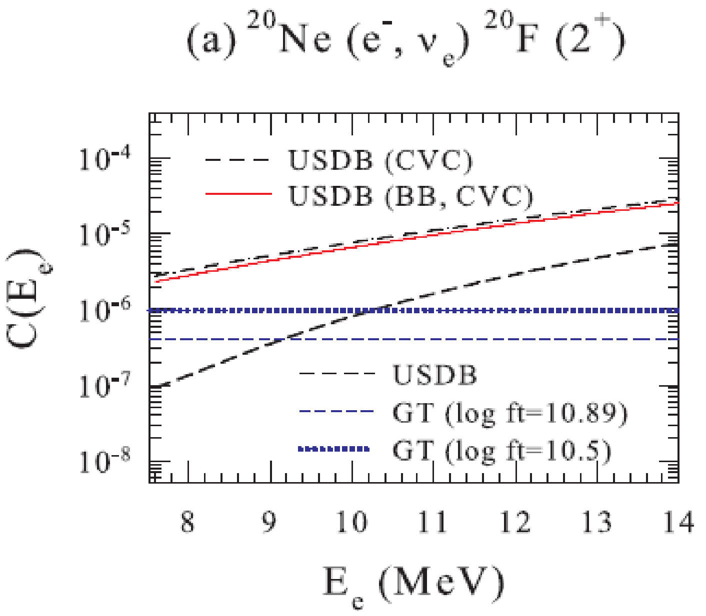

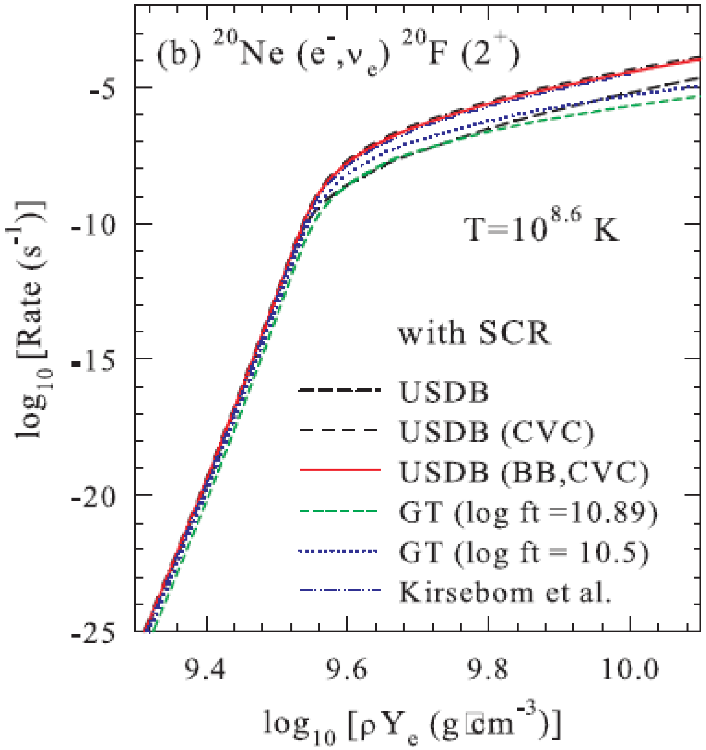

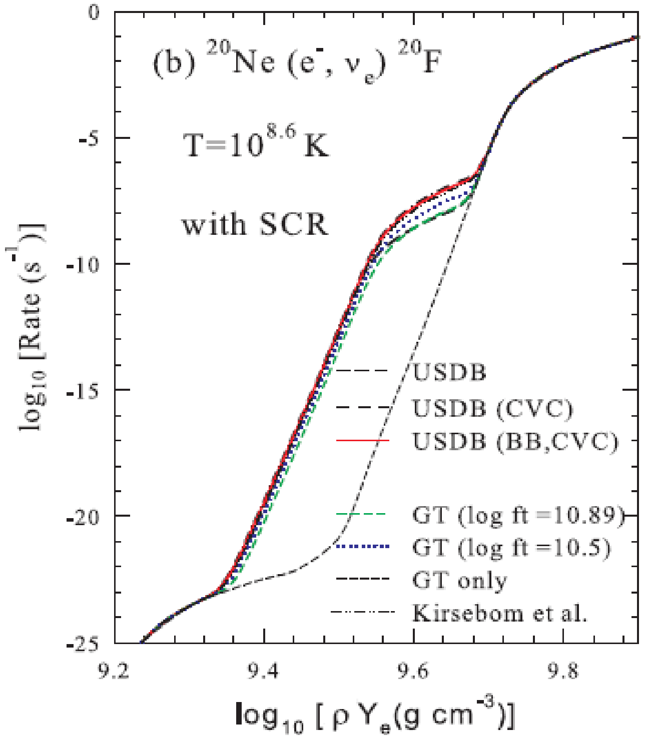

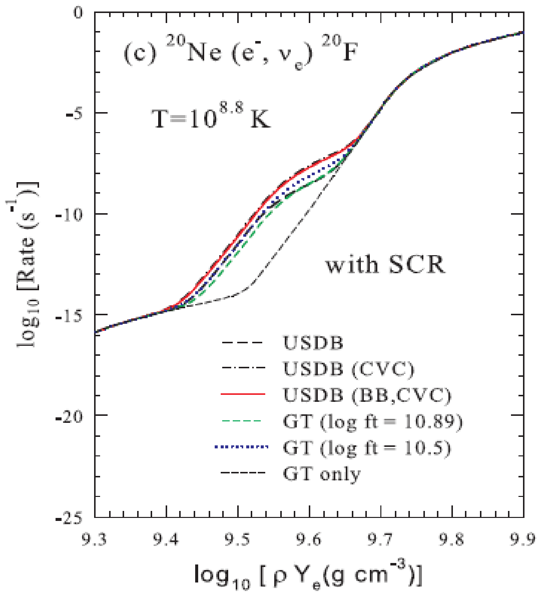

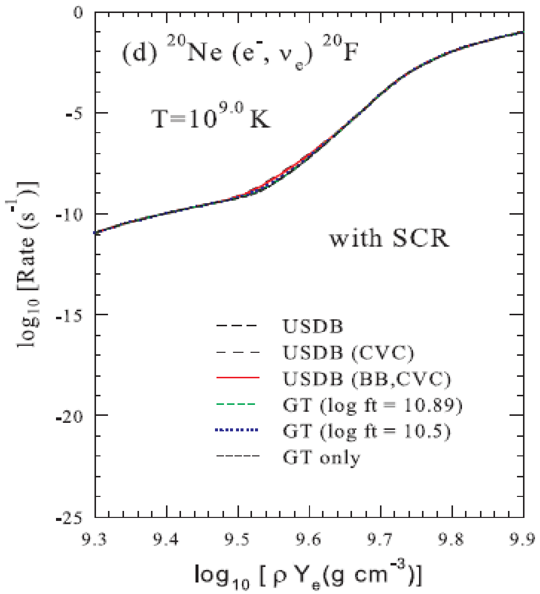

Kirsebom et al., *Phys. Rev.* C 100 (2019) 065805 .
Phys. Rev. Lett. 123 (2019) 262701

<2+|| r^2 Y^2 || 0+>: fitted to exp. (B(E2) value

T. Suzuki, S. Zha, S.-C. Leung, and K. Nomoto,
Astrophysical J. 881 (2019) 64

Heating of ONeMg core by double e-capture processes

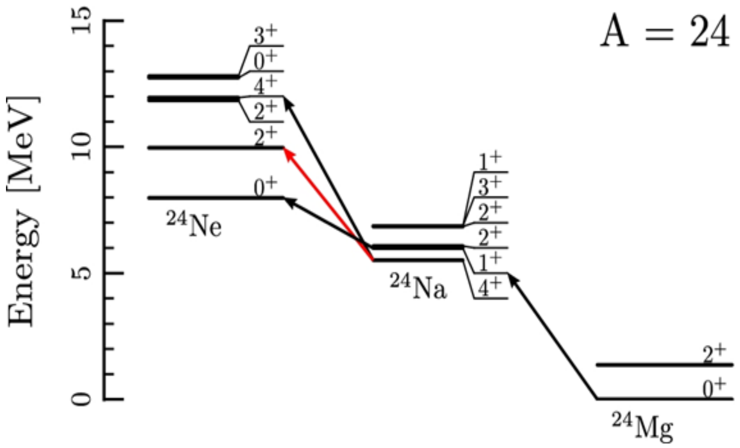

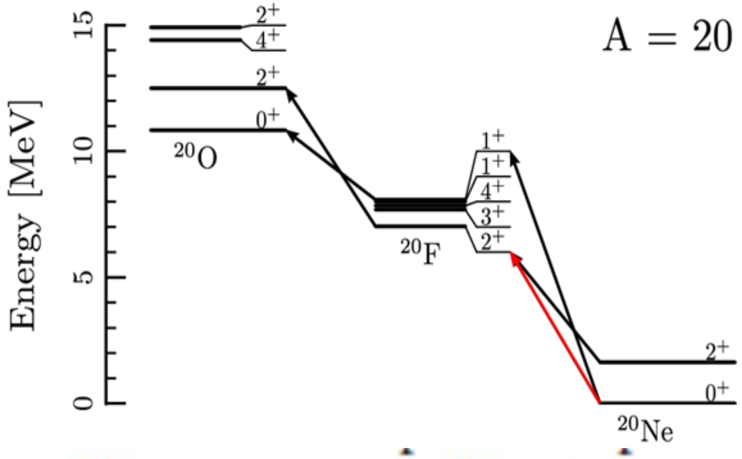

$^{24}\mathrm{Mg}\,(e^-,\nu_e)\ ^{24}\mathrm{Na}\,(e^-,\nu_e)\ ^{24}\mathrm{Ne}$ $\quad$ $^{20}\mathrm{Ne}\,(e^-,\nu_e)\ ^{20}\mathrm{F}\,(e^-,\nu_e)\ ^{20}\mathrm{O}$

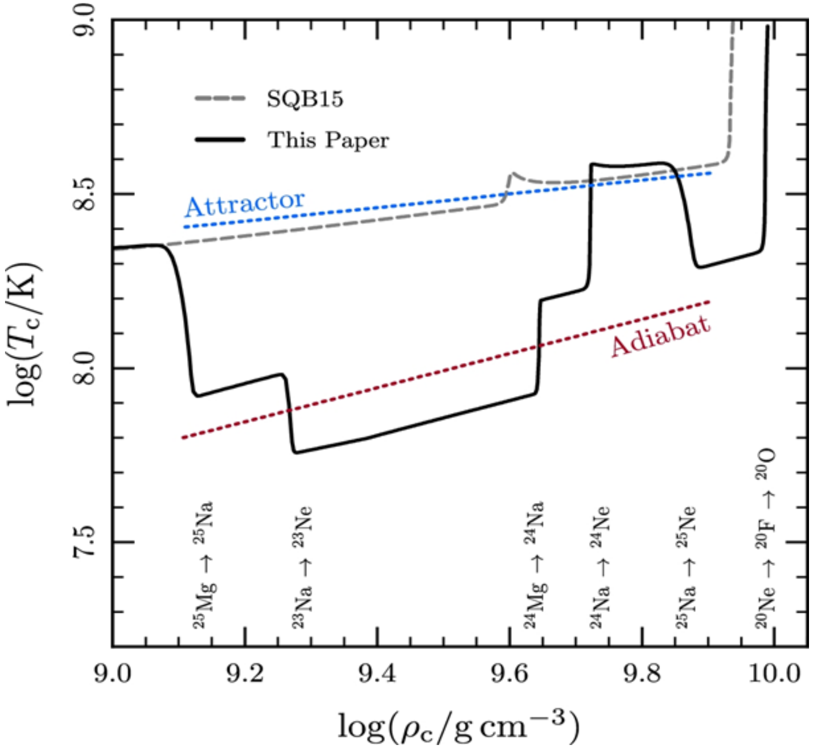

with the second-forbidden tr.

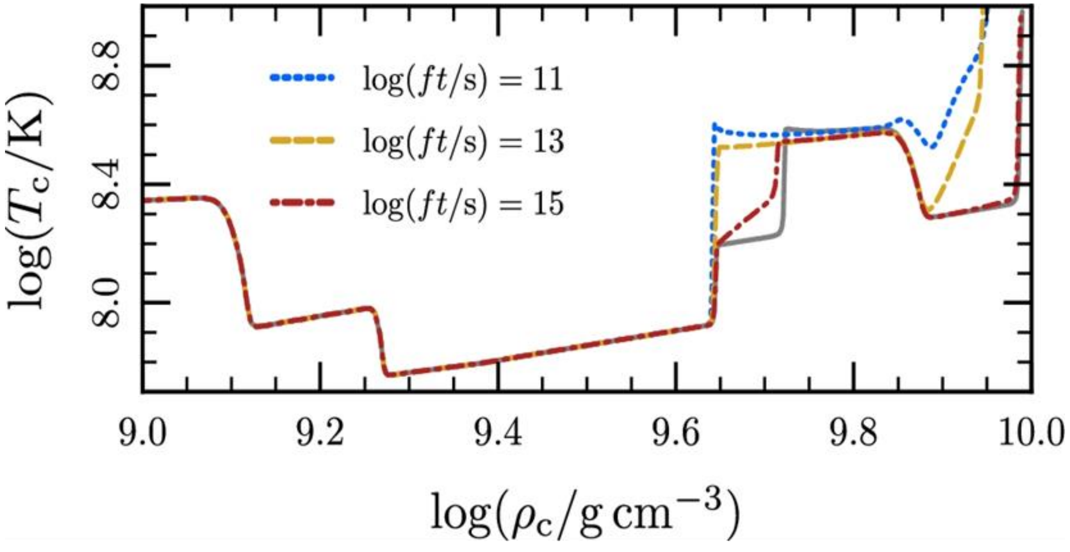

Schwab et al., MNRAS (2017)

Oxygen ignition: energy generation = ν energy loss

$\log(\rho_{c,ign}) = 9.96 - 10.0$

Heating time scale of local oxygen burning

$= C_p T/\varepsilon_{burn\_O} = 10^{7-8}$ s

>> dyn. time scale (~0.04 s) at $\rho = 10^{10}$g/cm^3

(Y_e reduction by e-capture on p)

Oxygen deflagration occurs at

$\rho_{c,def} > \rho_{c,ign}$

due to convection effects.

Oxygen burning occurs at

log (T/K)~ 9.3

→ $\rho_{c,def}$ is estimated

$\rho_{c,def} > 10.10$ *

$\rho_{c,def} = 10.2$ **

* Zha et al., ApJ 886, 22(2019)

** Takahashi et al., ApJ 871, 153 (2019)

Zha et al.

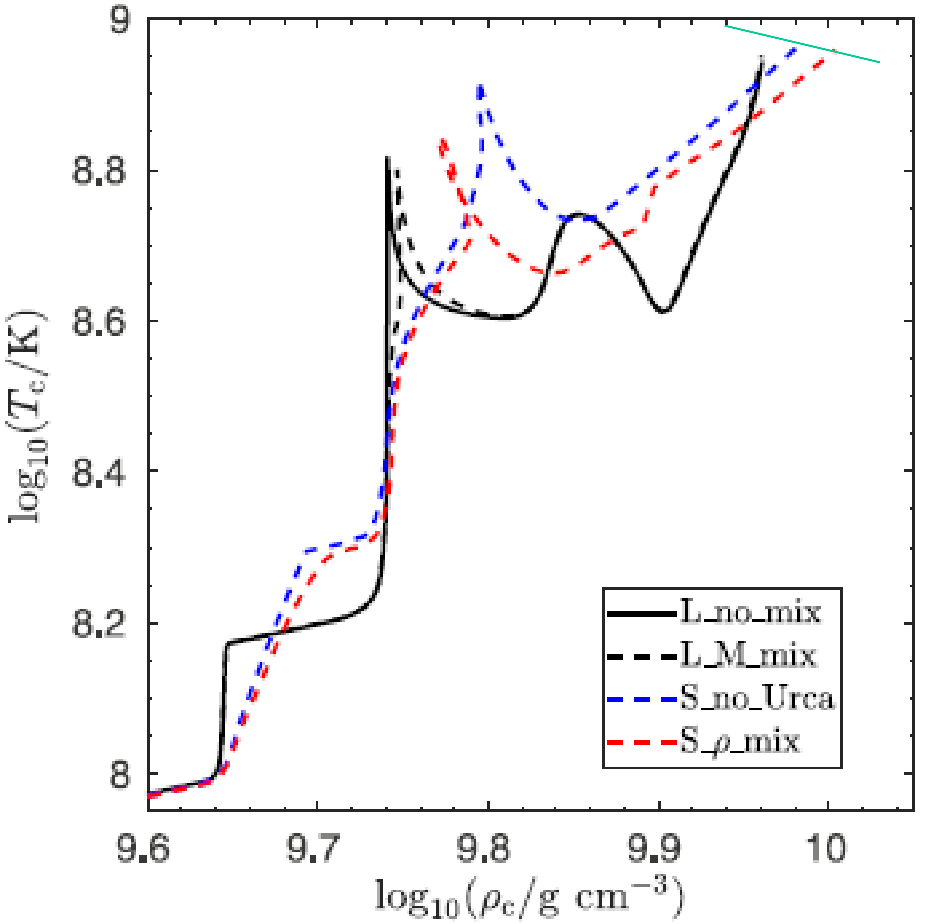

Figure 5. Evolution of the accreting ONeMg core in the central density–temperature plane for different treatments of the convection. Here "L" stands for the Ledoux criterion, and "S" stands for the Schwarzschild criterion. The additional model nomenclature is explained in the main text.

Explosion-collapse bifurcation

Fate of the ONeMg core

1. Thermonuclear explosion + ONeFe WD (white dwarf)
2. Collapse by ECSN + NS (neutron star)

2D hydrodynamical simulation for the propagation of the oxygen deflagration wave
(Zha, Leung, Suzuki and Nomoto, ApJ 886, 22 (2019))
e-capture rates: GT with USDB, 2^{nd}-forbidden with USDB (without CVC for E2)

e.g. Central density evolution of models with log ($\rho_{c,\,def}$ /g cm^{-3}) = 9.96, 9.98, 10.0

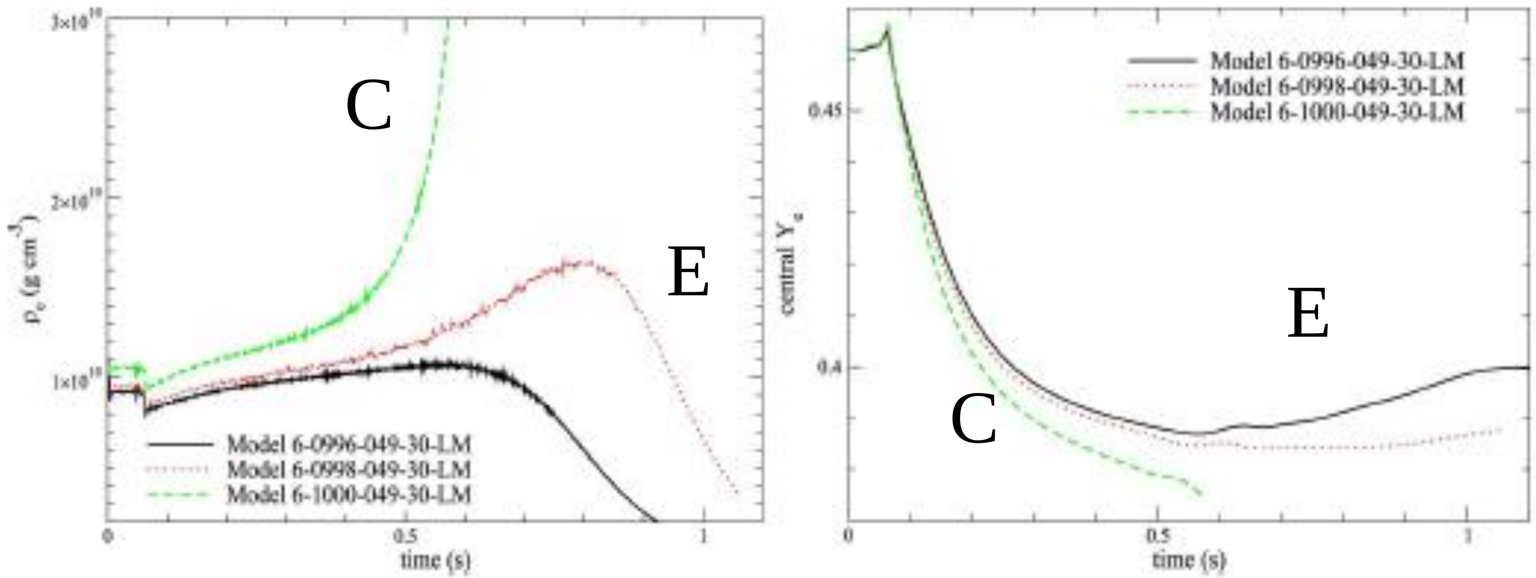

Explosion-Collapse bifurcation

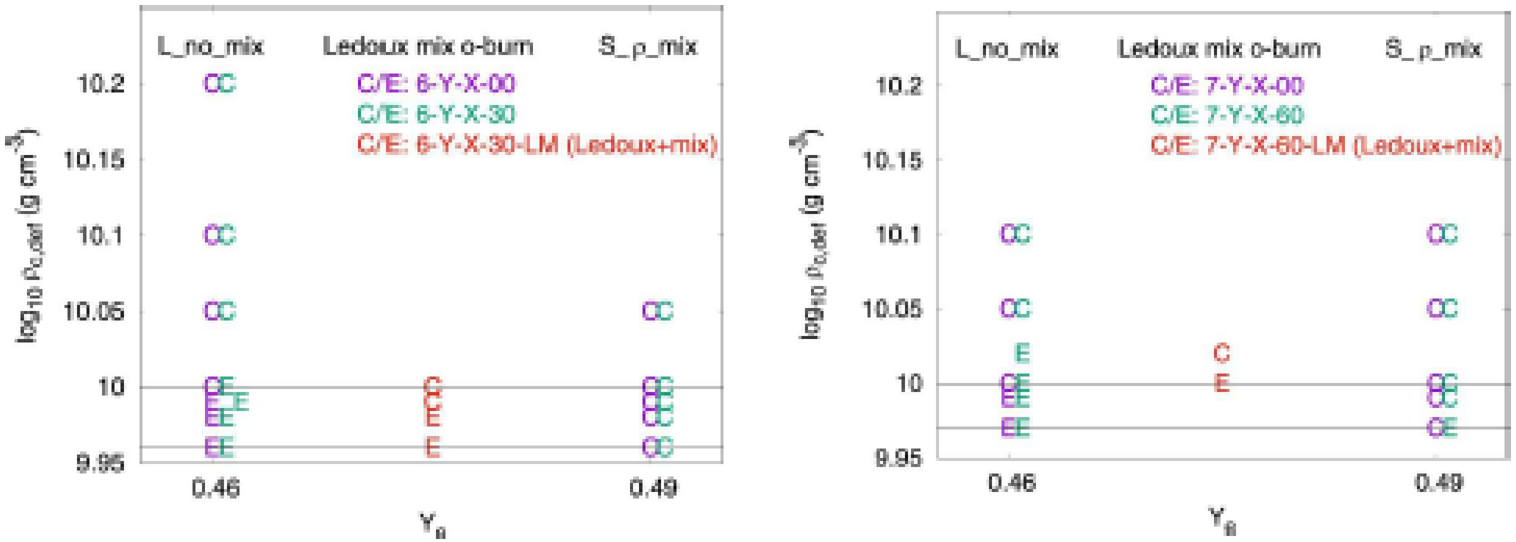

Explosion-collapse bifurcation diagram as a function of $\rho_{c,def}$ and the initial Y_e distribution for two Ledoux models and one Schwartzschild model. Here "E" and "C" stand for "explosion" and "collapse", respectively. Left (right) panel corresponds to the case of mass accretion rate of 10^{-6} (10^{-7}) $M_\odot$ yr^{-1}. From Zha et al, ApJ 886, 22 (2019)

$$\log(\rho_{crit}\,/\mathrm{gcm}^{-3}) = 10.01$$

$$\rho_{crit} > \rho_{c,def} \quad \rightarrow \quad \text{explosion}$$

$$\rho_{crit} < \rho_{c,def} \quad \rightarrow \quad \text{collapse}$$

$\rho_{c,def} \approx$10.1-10.2 $\rightarrow$ Collapse ECSN+NS

Cf. Jones et al., Kirsebom et al.

Jones et al., Astronomy and Astrophyics 622, A74 (2019)

Kirsebom et al., PRL 129, 262701 (2019)

- 3D hydrodynamical simulations
- e-capture rate for the 2nd-forbidden transition:
  USDB (CVC, BB) in Kirsebom et al.
  Taken as allowed GT with log ft = 10.5 in Jones
- Convection effects are taken to be mild.

$$\rho_{c,def} \approx \rho_{c,ign} \approx 9.96 - 9.97$$

$\rightarrow \rho_{crit} > \rho_{c,def}$

$\rightarrow$ thermonuclear explosion with ONeFe WD

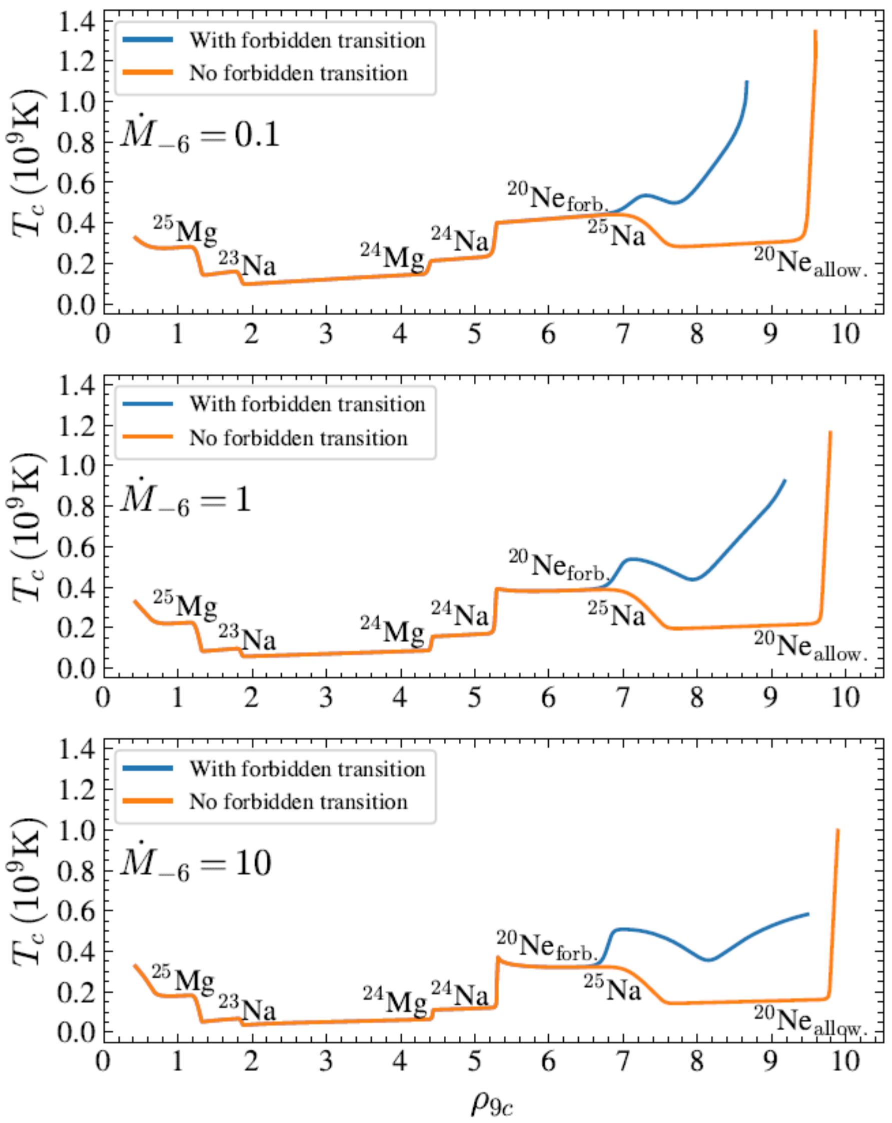

Summary

1. Weak rates for the Urca pair, ^{31}Mg-^{31}Al, are evaluated by an effective interaction obtained by the EKK method in sd-pf shell.
   Structure of ^{31}Mg is successfully described with energy levels consistent with the experimental data, which leads to a nuclear Urca process.

2. Spin-dipole strengths and e-capture rates are evaluated for ^{78}Ni by shell-model calculations with pf-sdg shell configurations. Use of full pf-sdg space is important to fulfill the spin-dipole sums.
   Comparison of SM results with RPA and the effective rate formula is made.
   Effects of un-blocking of GT strengths are not considered here.

E. Litvinova and C. Robin, *Phys. Rev.* C 103 (2021) 024326

S. Giraud, R. G. T. Zegeres, B. A. Brown et al., arXiv:2112.01626 (2021).

A. A. Dzhioev et al., PRC 81 (2010) 01584.

3. Weak rates for the second-forbidden transition in ^{20}Ne are evaluated by the multipole expansion method by Walecka as well as the Behrens-Buhring method.
Importance of the CVC relation in the E2 matrix element is pointed out.
The difference of the rates between Walecka and Behrens-Buhring is minor in the present case, as far as the CVC relation is taken into account.

Final fate of ONeMg cores in 8-10$M_\odot$ stars, collapse or thermonuclear explosion, is discussed.
Need to understand more clearly the evolution from the oxygen ignition (at the end of the MESA calculations) till the beginning of the deflagration by taking into account the semi-convection and convection.
Use of the rates with full inclusion of the CVC relation is desired .
More observational and theoretical studies are necessary to draw a definite conclusion on the final fate of the stars with 8-10 $M_\odot$.

Collaborations with

K. Nomoto, H. Toki, for sd-shell
K. Mori, T. Kajino, M. Famiano, A. B. Balantekin, for pf-shell
N. Tsunoda, N. Shimizu, T. Otsuka, for sd-pf shell
N. Shimizu, Y. Tsunoda, T. Otsuka, for pf-sdg shell
S. Zha, S.-C. Leung, K. Nomoto, for ^{20}Ne

Supplementary slides

- β-decay: ^{20}F ($2^+_{g.s.}$) ⟶ ^{20}Ne ($0^+_{g.s.}$) + e^- + ν_e

log ft = 10.70 USDB (CVC)

10.65 USDB (BB), 10.86 USDB (BB) with exp. B(E2)

10.89(11) Exp. Kirsebom et al. PRL 123, 262701 (2019)

$$ft = \ln 2 \frac{I}{\lambda^\beta} \qquad I = \int_{m_e c^2}^{Q} E_e p_e c (Q - E_e)^2 F(Z+1, E_e)(1 - f(E_e)) dE_e.$$

$$\lambda^\beta(T) = \frac{V_{ud}^2 g_V^2 c}{\pi^2 (\hbar c)^3} \int_{m_e c^2}^{Q} S(E_e, T) E_e p_e c (Q - E_e)^2 (1 - f(E_e)) dE_e$$

$$S(E_e, T) = \sum_i \frac{(2J_i + 1) e^{-E_i/kT}}{G(Z, A, T)} \sum_f \frac{G_F^2}{2\pi} F(Z+1, E_e) C_{f,i}(E_e)$$

$$\begin{aligned}
C_{f,i}(E_e) &= \int \frac{1}{4\pi} d\Omega_\nu \int d\Omega_k \frac{1}{2J_i + 1} \Big(\sum_{J \geq 1} \{ (1 - (\hat{\vec{\nu}} \cdot \hat{\vec{q}})(\vec{\beta} \cdot \hat{\vec{q}}) [|\langle J_f || T_J^{mag} || J_i \rangle|^2 \\
&+ |\langle J_f || T_J^{elec} || J_i \rangle|^2] + 2\hat{\vec{q}} \cdot (\hat{\vec{\nu}} - \vec{\beta}) Re \langle J_f || T_J^{mag} || J_i \rangle \langle J_f || T_J^{elec} || J_i \rangle^* \} \\
&+ \sum_{J \geq 0} \{ (1 - \hat{\vec{\nu}} \cdot \vec{\beta}) + 2(\hat{\vec{\nu}} \cdot \hat{\vec{q}})(\vec{\beta} \cdot \hat{\vec{q}}) |\langle J_F || L_J || J_i \rangle|^2 + (1 + \hat{\vec{\nu}} \cdot \vec{\beta}) |\langle J_f || M_J || J_i \rangle|^2 \\
&- 2\hat{\vec{q}} \cdot (\hat{\vec{\nu}} + \vec{\beta}) Re \langle J_f || L_J || J_i \rangle \langle J_f || M_J || J_i \rangle^* \} \Big),
\end{aligned}$$

$\vec{q} = \vec{k} + \vec{\nu}$, $q_0 = E_e + \nu = Q + E_i - E_f$ is positive ($Q = 7.535$ MeV)

Comparison of e-capture rates: KB3G vs GXPF1A

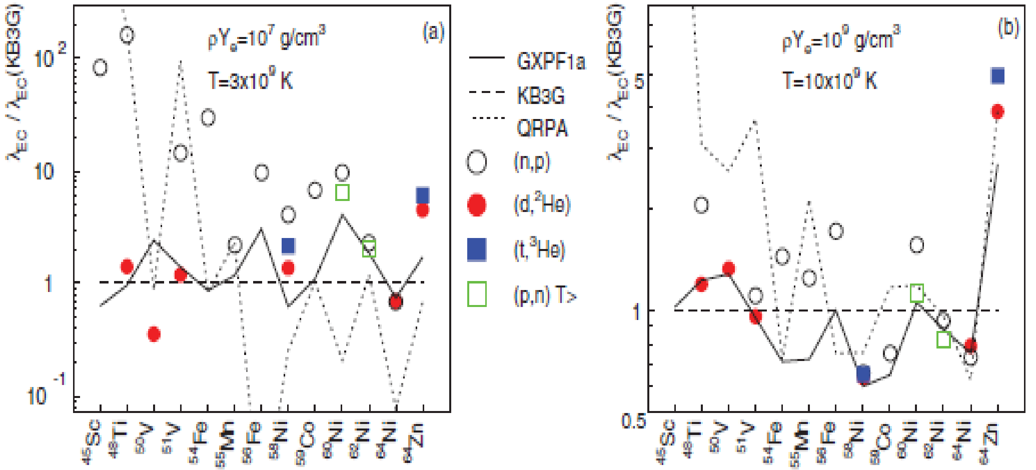

Cole et al., PR C86, 015809 (2012)

e-capture rates: GXP;
GXPF1J (21≤Z≤32) and KBF (other Z)

GXP:W7 (fast deflagration)

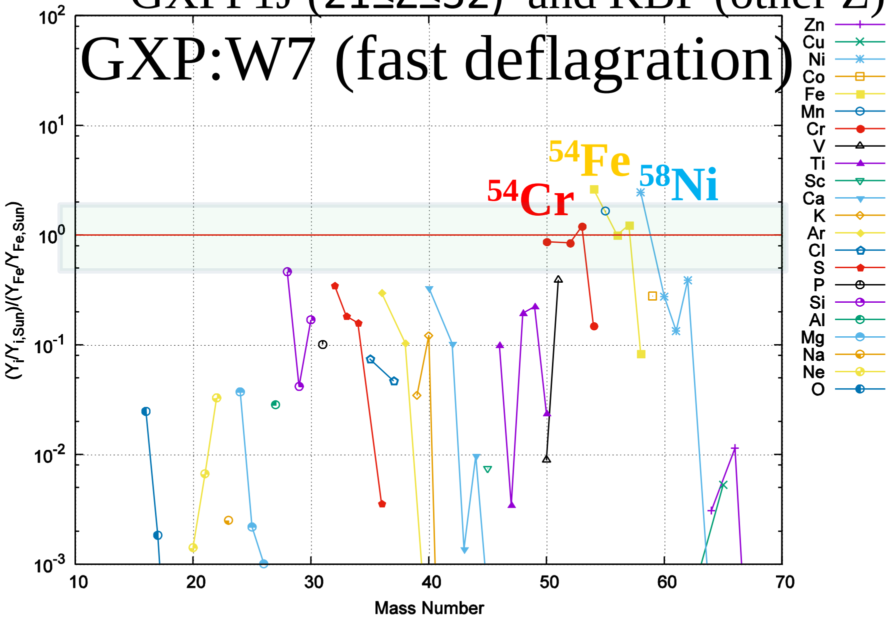

GXPF1J
cf. KBF
KB3G

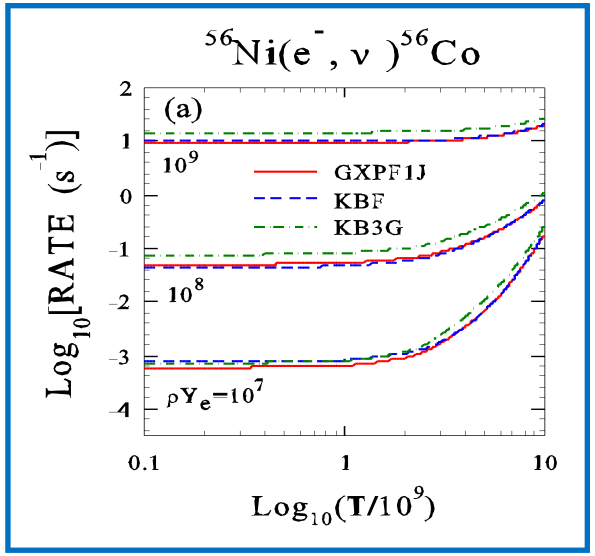

GXP: WDD2 (slow deflagration + detonation)

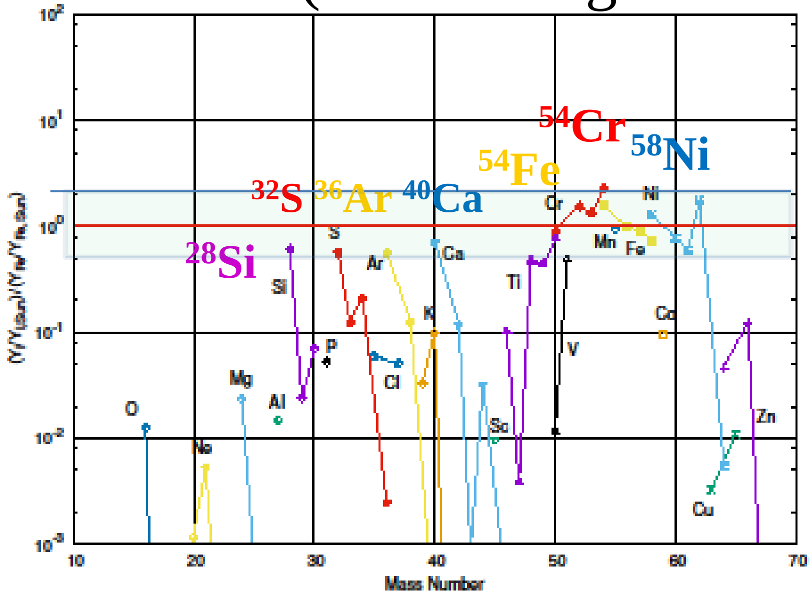

Mori, Famiano, Kajino, Suzuki, Hidaka, Honma, Iwamoto, Nomoto, Otsuka, ApJ. 833, 179 (2016)

Coulomb corrections: screening effects

1. Screening effects of electrons

$V(r)$ with screening effects of relativistic degenerate electron liquid

$$V(r) = -\frac{Ze^2}{2\pi^2}\int \frac{e^{i\vec{k}\vec{r}}}{k^2\epsilon(k,0)}d^3k = -\frac{Ze^2 2k_F}{2k_F r}\frac{2}{\pi}\int \frac{\sin(2k_F qr)}{q^2\epsilon(q,0)}dq.$$

$$V_s(r) = V(r) - \left(-\frac{Ze^2}{r}\right) = Ze^2(2k_F)J,$$

Juodagalvis et al., Nucl. Phys. A 848, 454 (2010).
Itoh et al, Astrophys. J. 579, 380 (2002).

Vs(0)>0 → reduce (enhance) e-capure (β-decay) rates

2. Change of threshold energy

$$\Delta Q_C = \mu_C(Z-1) - \mu_C(Z),$$

$\mu_C(Z)$ =the correction of the chemical potential of the ion with Z

ΔQ_c → reduce e-capture rates & enhance β-decay rates

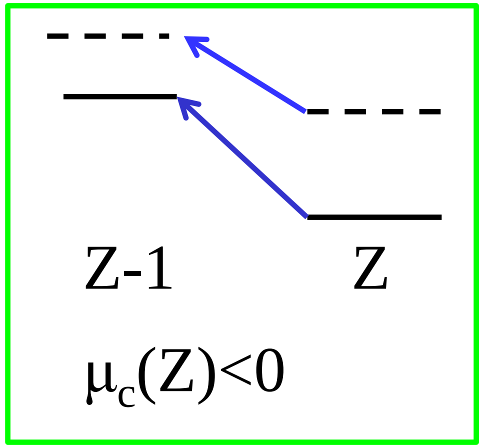

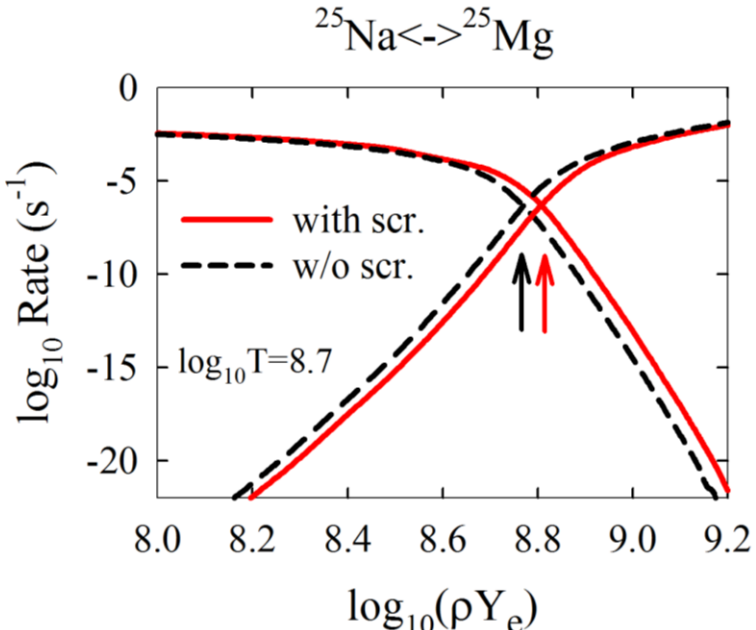

Slattery, Doolen, DeWitt, Phys. Rev. A26, 2255 (1982).
Ichimaru, Rev. Mod. Phys. 65, 255 (1993).

$\rho Y_e = 8.78 \rightarrow 8.81$

URCA density → higher density region

Screening Effects on Electron Capture Rates and Type Ia Supernova Nucleosynthesis

Kanji Mori[1,2,8], Toshio Suzuki[2,3], Michio Honma[4], Michael A. Famiano[2,5], Toshitaka Kajino[1,2,6], Motohiko Kusakabe[6], and A. Baha Balantekin[2,7]

The Astrophysical Journal, 904:29 (6pp), 2020

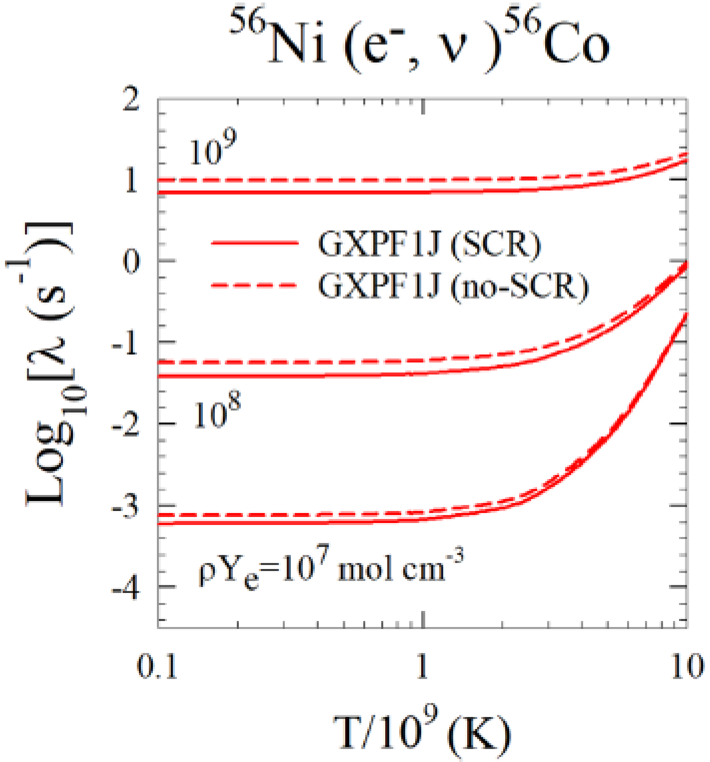

Figure 1. Comparison of calculated *e*-capture rates for ^{56}Ni (e^-, ν) ^{56}Co obtained with the GXPF1J at densities $\rho Y_e = 10^7$, 10^8, and 10^9 mol cm^{-3} for temperatures $T = 10^8$–10^{10} K. Solid and dashed curves denote the rates with and without the screening effects, respectively.

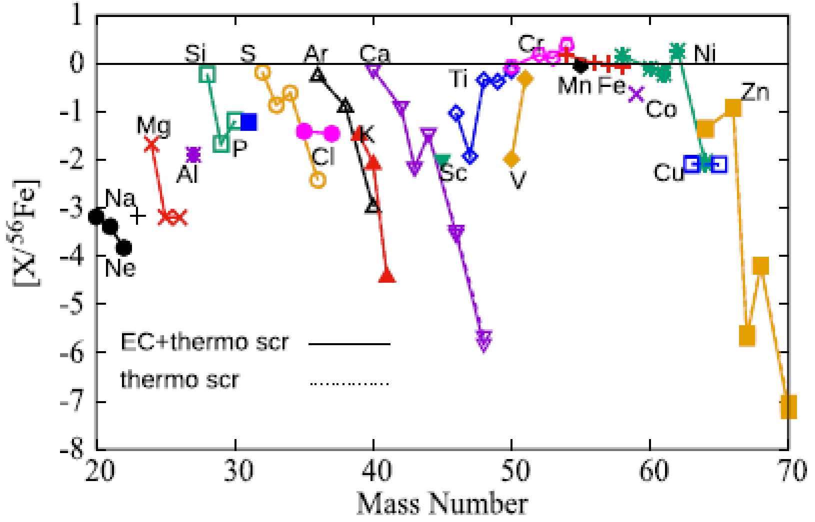

Figure 7. Abundances normalized by the solar and ^{56}Fe abundances. The solid lines adopt screening on ECs and the broken lines do not. WDD2 is adopted as an SN Ia model.

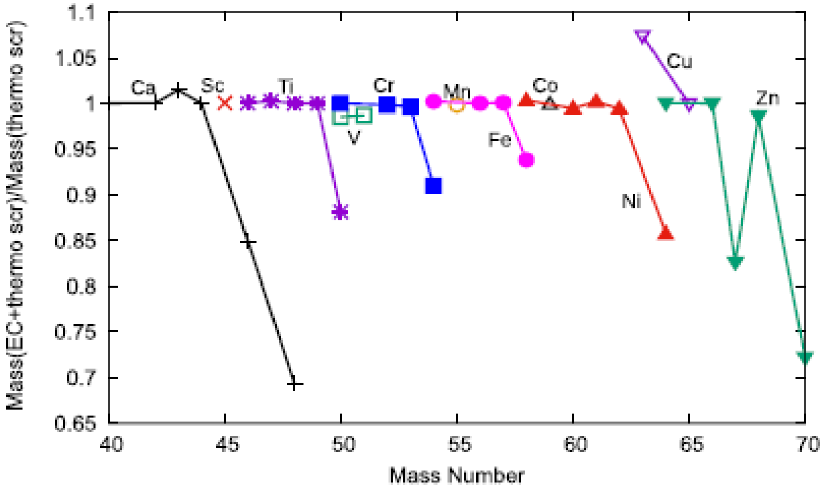

Figure 6. Abundance ratios between the cases with and without screening on ECs. WDD2 is adopted as an SN Ia model.

Chiral effective NN interaction

Chiral Effective Field Theory: Nuclear Forces

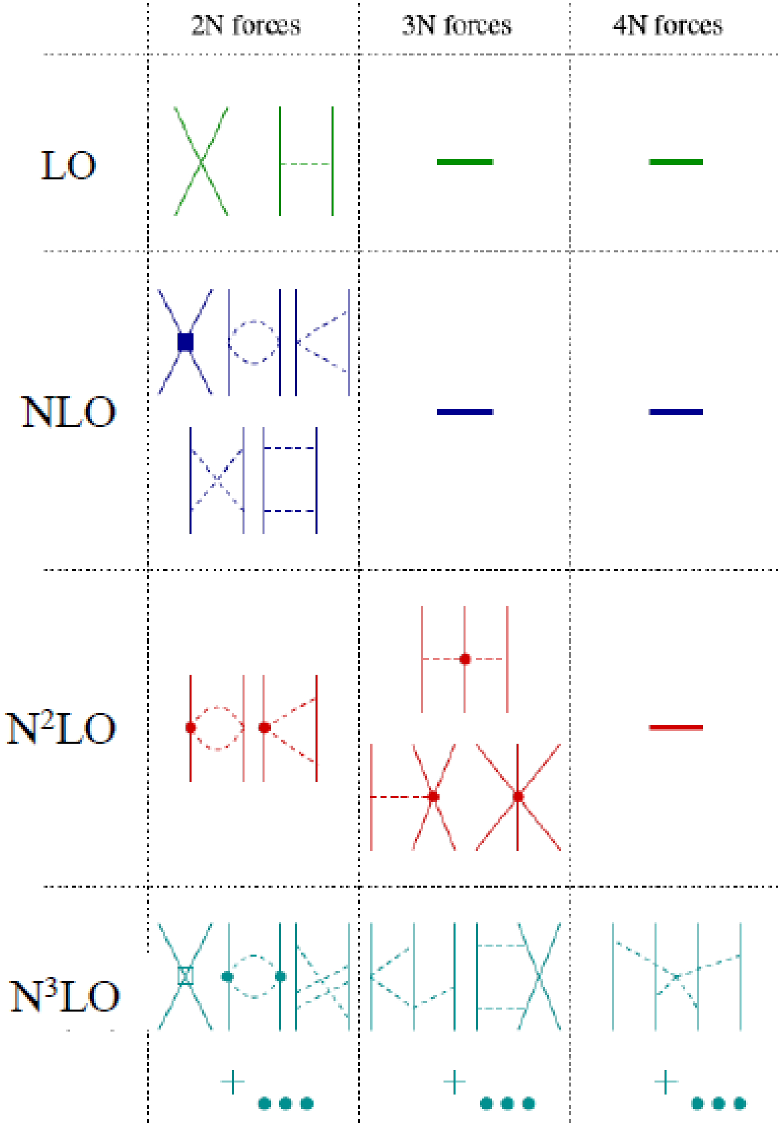

Nucleons interact via pion exchanges and contact interactions

expansion in m_π/Λ, p/Λ

Hierarchy: $V_{NN} > V_{3N} > \ldots$

Consistent treatment of NN, 3N, … electroweak operators

Cf.

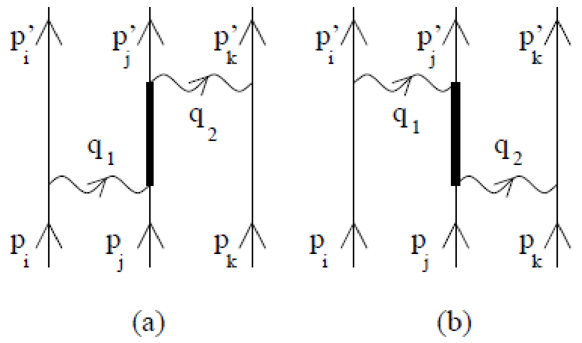

Δ-resonance

Weinberg, van Kolck, Kaplan, Savage, Wise, Epelbaum, Kaiser, Meissner,…